Measurements of hadron production in p-Pb collisions at LHCf

Gaku Mitsuka
(University of Florence, INFN Firenze, and JSPS fellow)
on behalf of the LHCf collaboration

LHCP conference, Columbia University
June 2-7, 2014

Outline

- Introduction and Physics motivation
- Very forward π^0 p_T spectra in p-Pb at 5.02 TeV (Neutron energy spectra in p-p at 7 TeV)
- (Preparation towards the 13 TeV operation)
- Summary

The LHCf collaboration

The LHCf collaboration involves ~30 members from 10 institutions.

The LHCf detectors

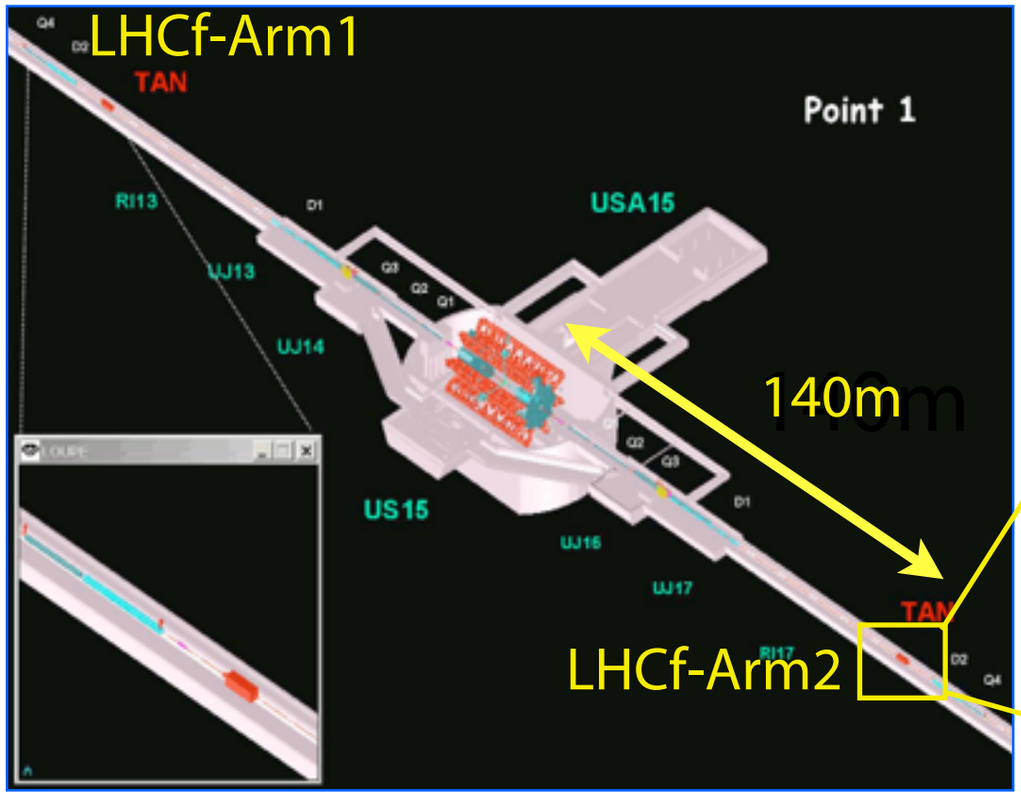

10(W)cm x 10cm(H) x 30cm(D)
Sampling calorimeter, $44X_0$, 1.6λ
Two-tower structure

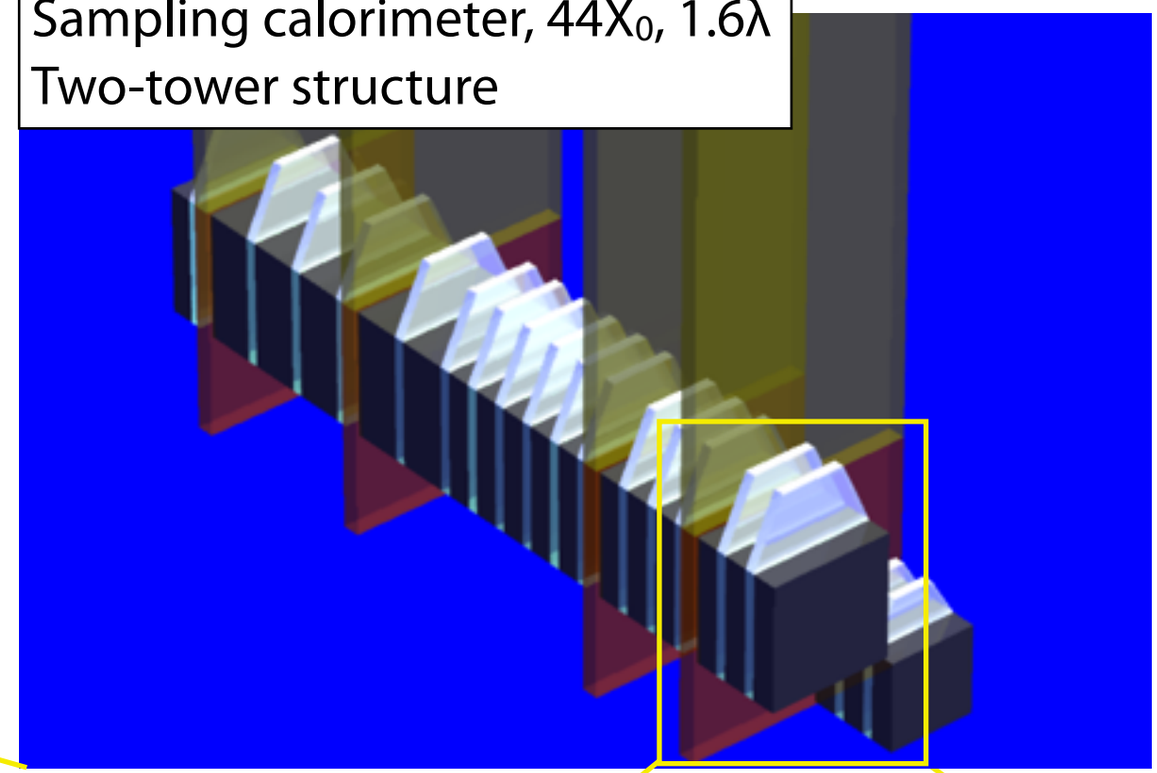

Position sensitive detector
Arm1 : Scintillation fibers
Arm2 : Silicon strip detector

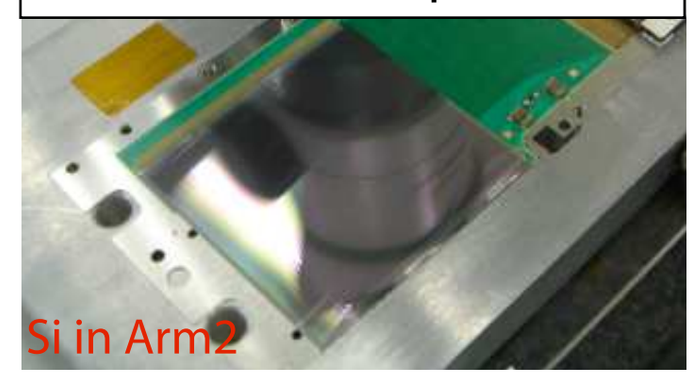

- Two independent detectors (Arm1 and Arm2) are located in TAN to measure the ***very forward particles***:
  - $\eta>8.7$ w/o crossing angle and $\eta>8.4$ with crossing angle
  - $p_T<1.0$GeV at $\sqrt{s}=7$TeV.
- Sampling calorimeter + position sensitive detector.
- Charged particles are swept away due to the D1 magnet, so we can only observe neutral particles (photon and neutron).
- Same detectors have been used since 2009.

Detector performances

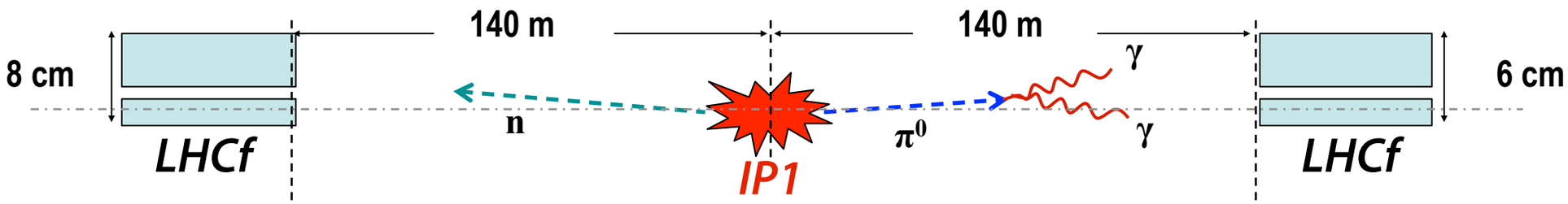

Hadronic shower (MC)

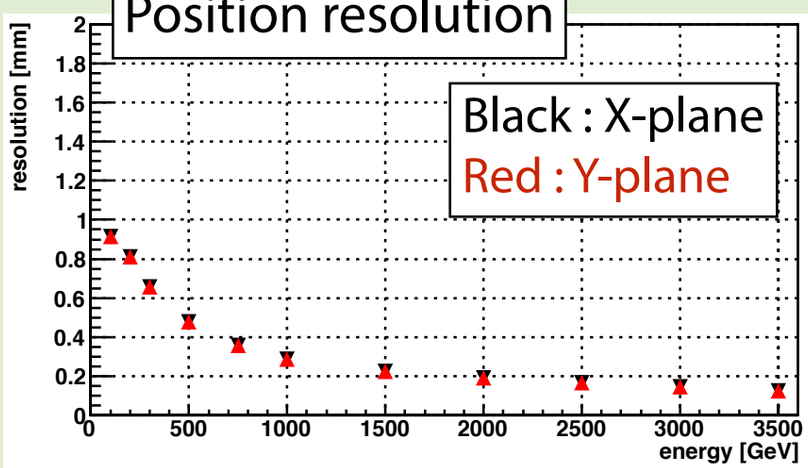

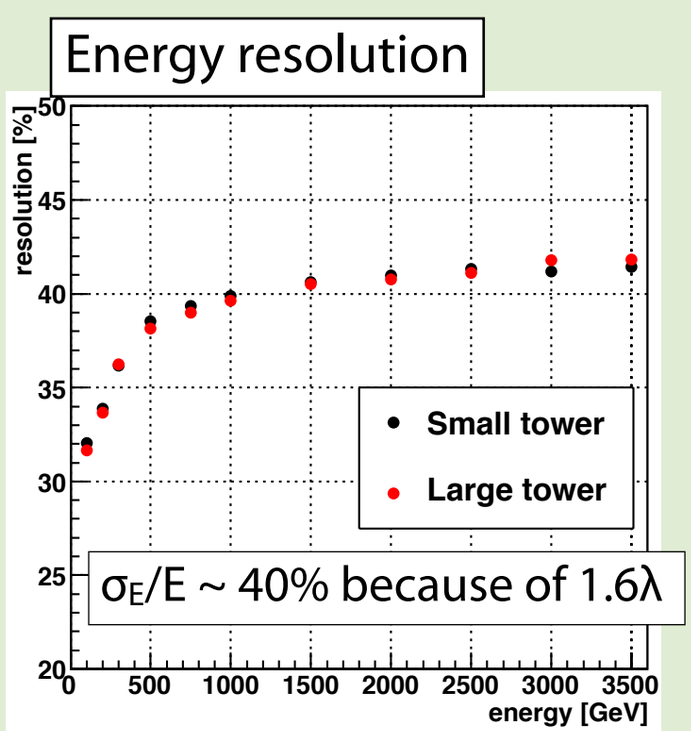

EM shower (MC)

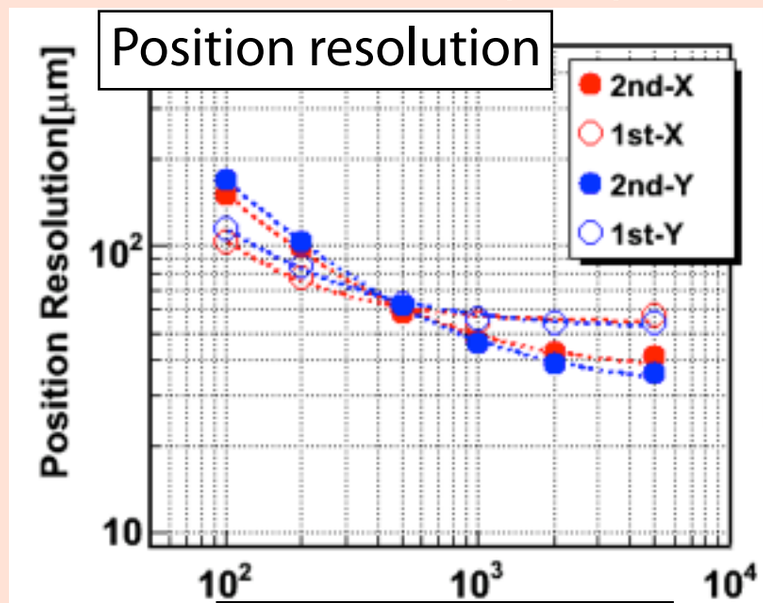

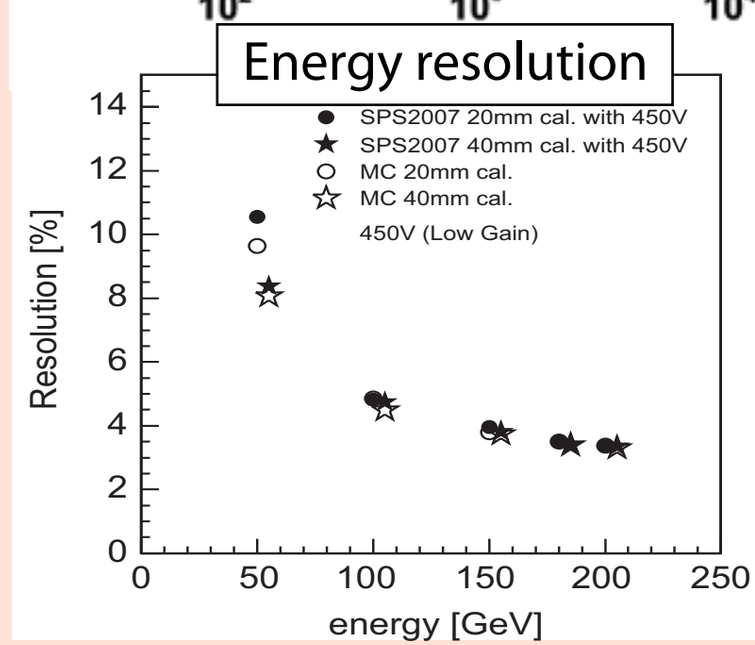

PID technique

400GeV photon

1TeV neutron

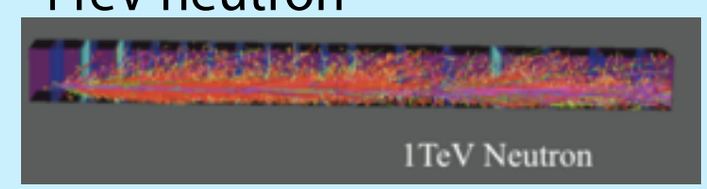

Identification of incoming particle by shower shape

π^0 reconstruction

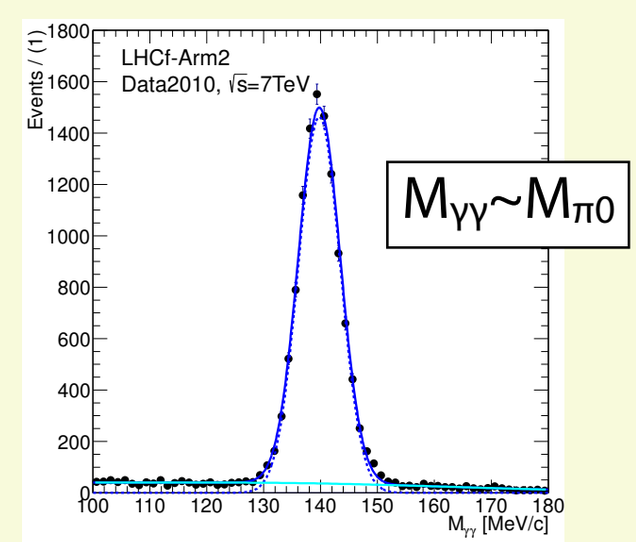

Physics motivation (cosmic ray point of view)

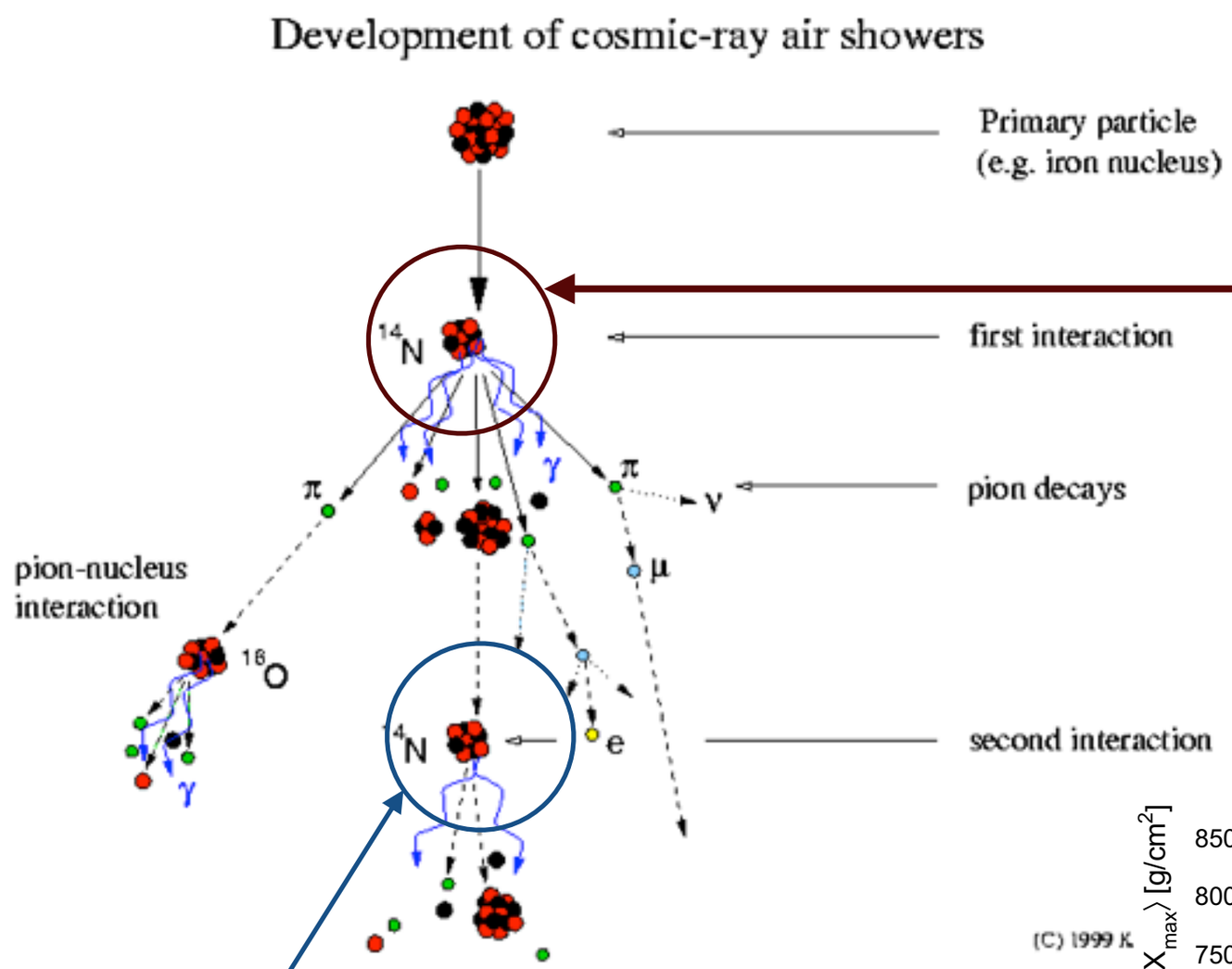

1. **Charge ratio** (e.g. NA61)
2. **Multiplicity**
   number of muons in air shower sensitive to mass composition

1. **Inelastic cross section** (by TOTEM)
   large → rapid development
   small → deep penetrating
2. **Inelasticity $k = 1 - p_{lead}/p_{beam}$** neutron (~leading baryon)
   large → rapid development
   small → deep penetrating
3. **Forward energy spectrum** photon or π^0
   softer → rapid development
   harder → deep penetrating
4. **Nuclear effects** p-Pb collisions
5. **Extrapolation to high energy** many data points
   precise measurements at lower energies are crucial

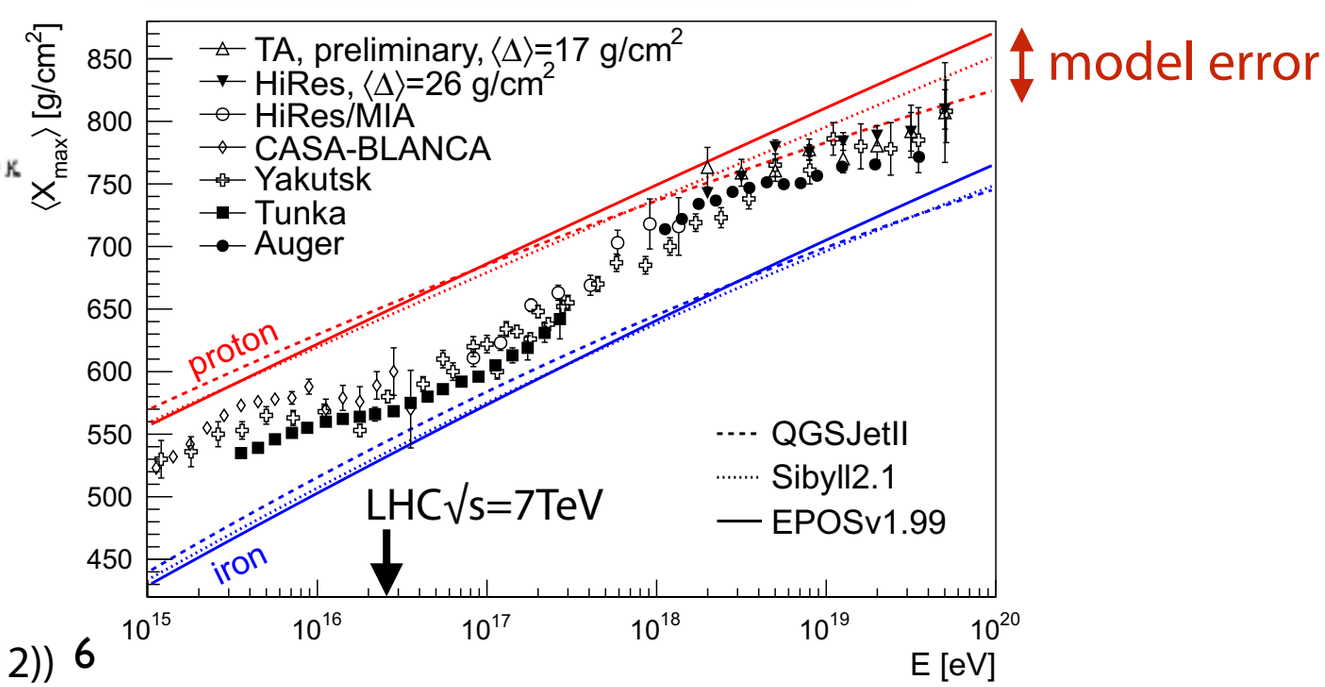

(Kampert and Unger, Astropartphys. 35, 660, (2012))

Physics and test beam analysis at LHCf

	Photon (EM shower)	Neutron (hadron shower)	π0 (EM shower)
Test beam at SPS	NIM. A 671, 129–136 (2012)	JINST 9 P03016 (2014)	
p-p at 900GeV	Phys. Lett. B 715, 298-303 (2012)		
p-p at 7TeV	Phys. Lett. B 703, 128–134 (2011)	Paper in preparation	Phys. Rev. D 86, 092001 (2012)
p-p at 2.76TeV			Submitted to Phys Rev. C arXiv:1403.7845, CERN-PH-EP-2014-059
p-Pb at 5.02TeV			

- LHC's analysis activity was first directed to the EM shower events for its simplicity.
- We show the analysis result of forward π^0s in p-Pb collisions.
- Note we have extended the activity to neutron event analysis based on improved tools.

Analysis on the other parts are ongoing.

π^0 event categories in p-Pb collisions

(Soft) QCD :
central and peripheral collisions

Ultra peripheral collisions :
virtual photon from rel. Pb collides a proton.

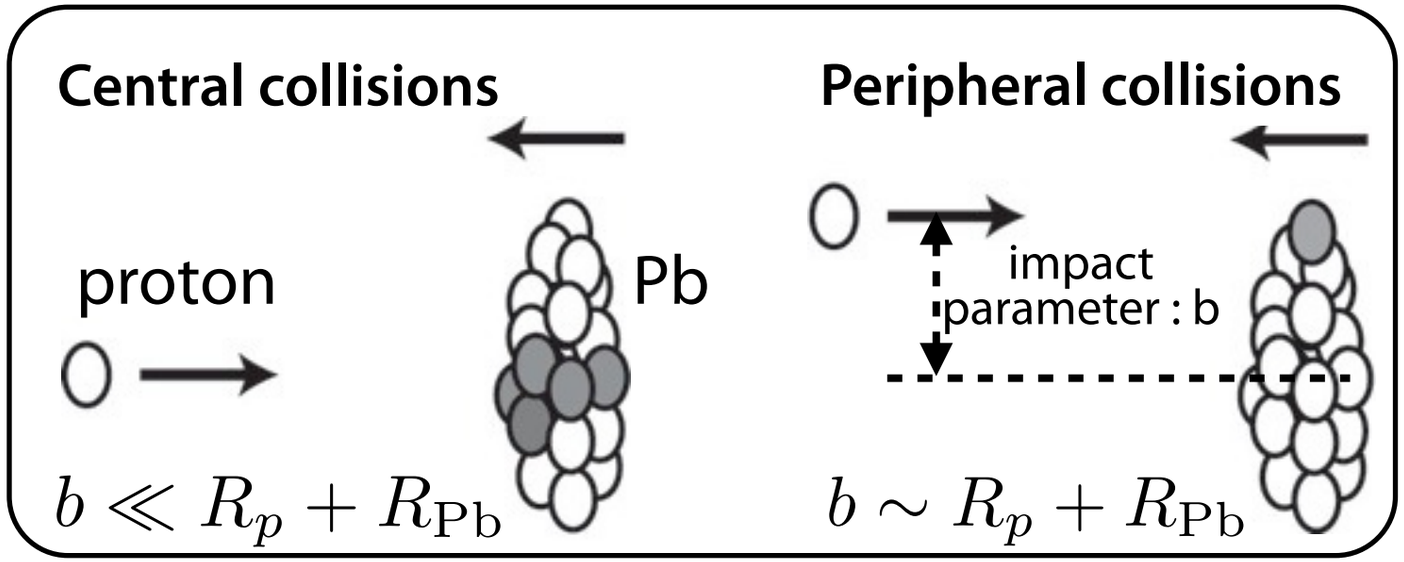

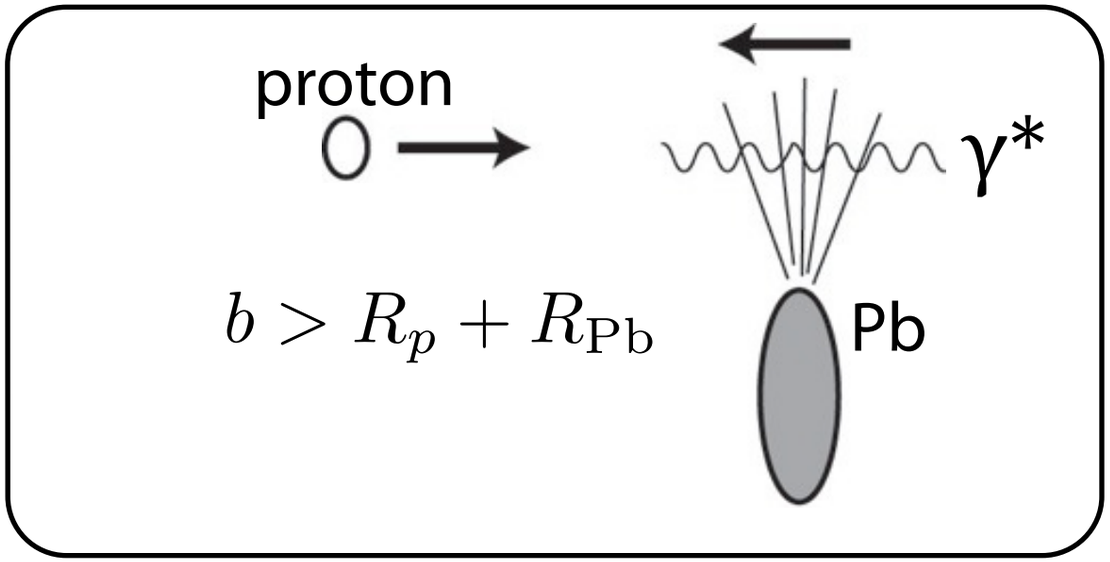

Momentum distribution of the UPC induced secondary particles is estimated as

1. energy distribution of virtual photons is estimated by the Weizsacker Williams approximation.
2. photon-proton collisions are simulated by the SOHIA model (E_γ > pion threshold).

] proton rest frame

3. produced mesons and baryons by γ-p collisions are boosted along the proton beam.

Dominant channel to forward π^0 is

$$\gamma + p \rightarrow \Delta(1232) \rightarrow p + \pi^0$$

About half of the observed π^0 may originate in UPC, another half is from soft-QCD.

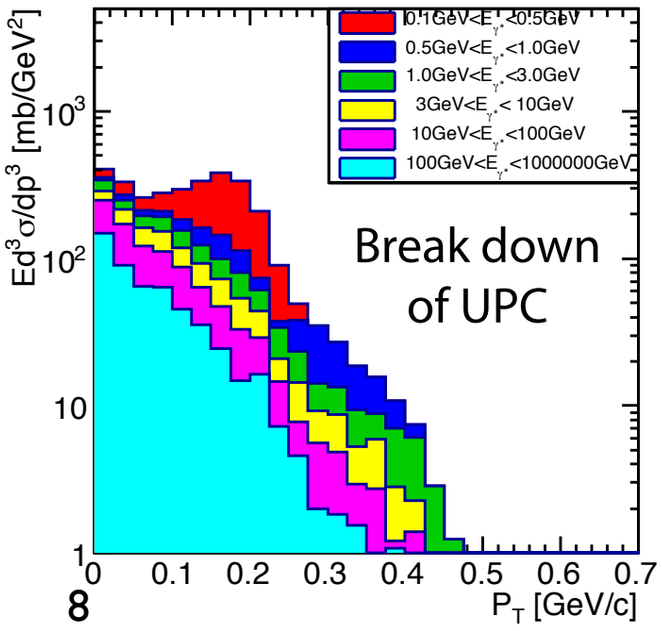

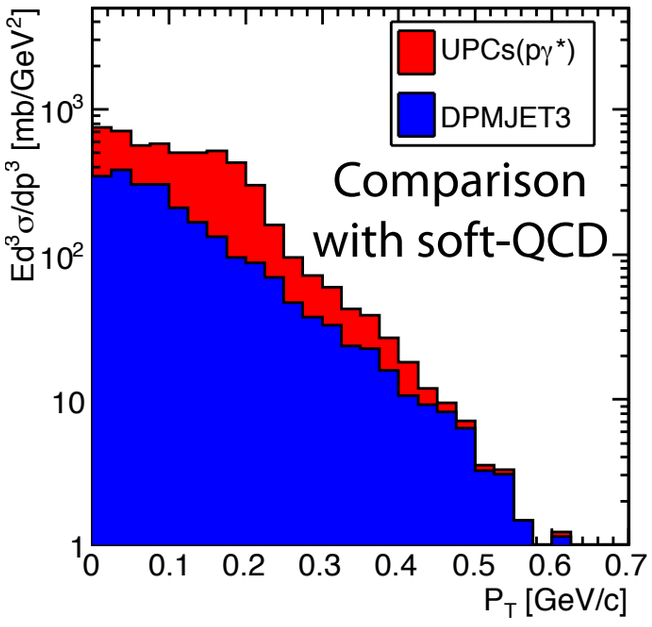

arXiv:1403.7845, CERN-PH-EP-2014-059

π^0 event reconstruction in p-Pb collisions

1. Search for two photons

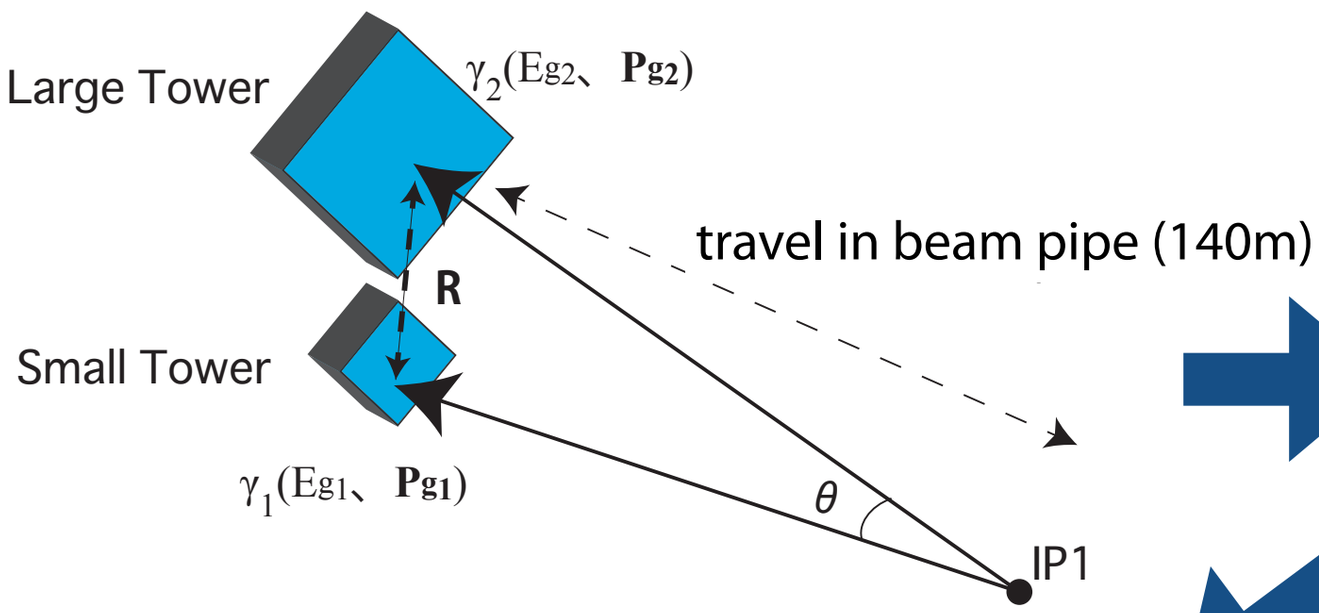

2. BG subtraction by sideband

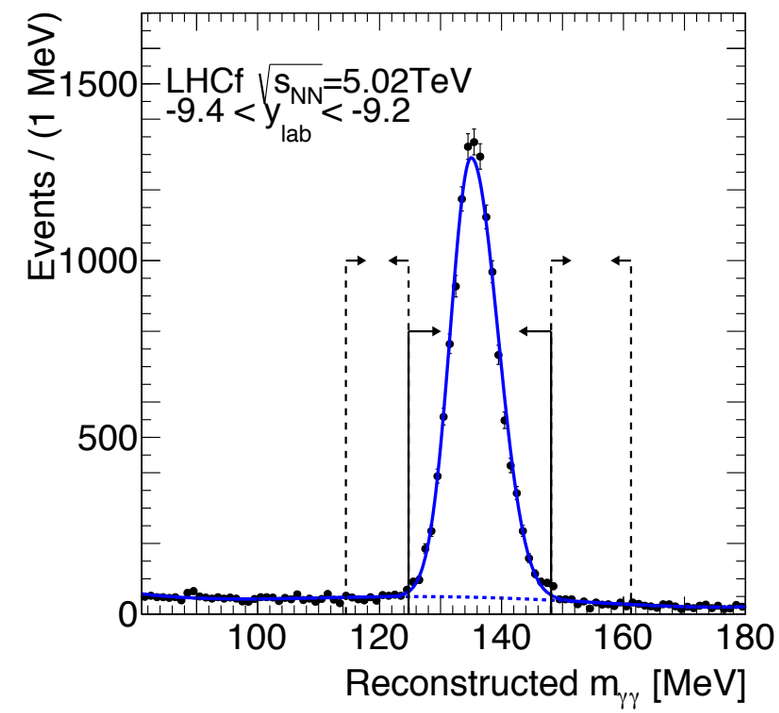

3. Unfolding the smeared p_T spectra and correction for geometrical inefficiency

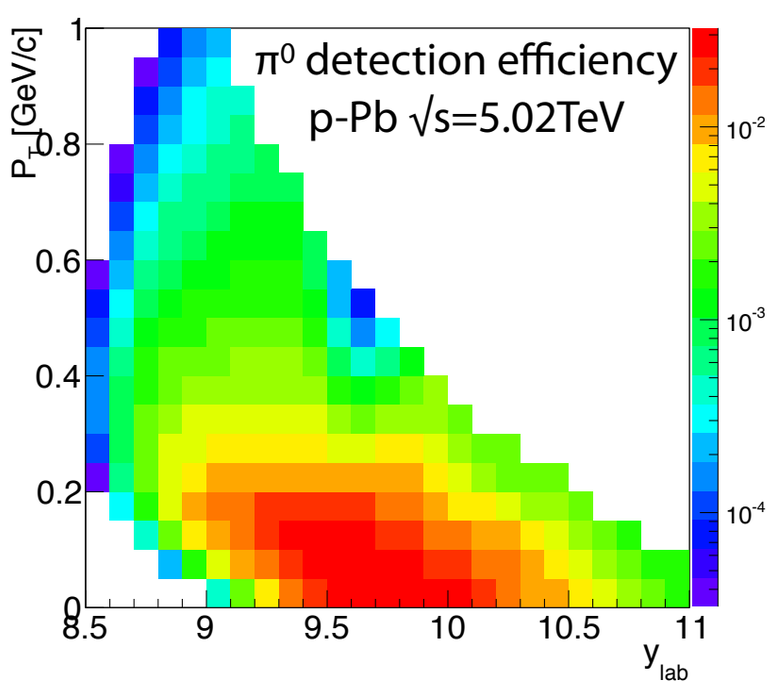

4. Subtraction of the UPC component

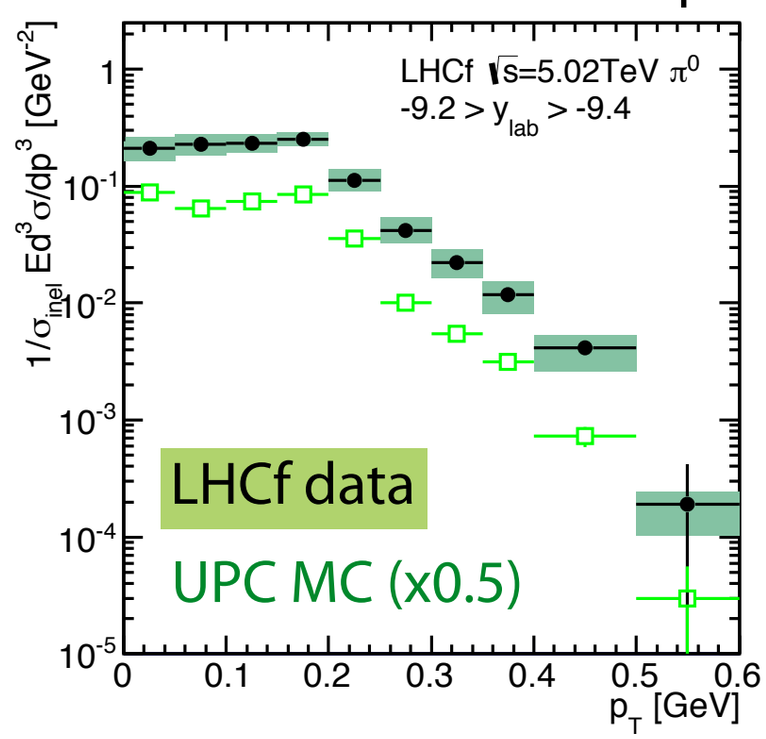

arXiv:1403.7845, CERN-PH-EP-2014-059

Derivation of π^0 p_T spectra in p-p at 5.02TeV

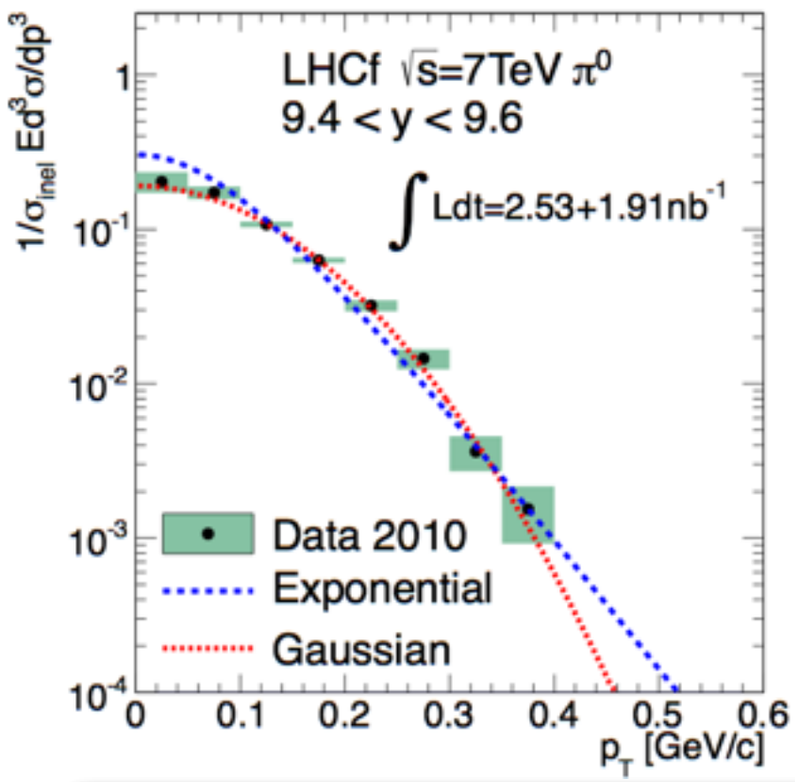

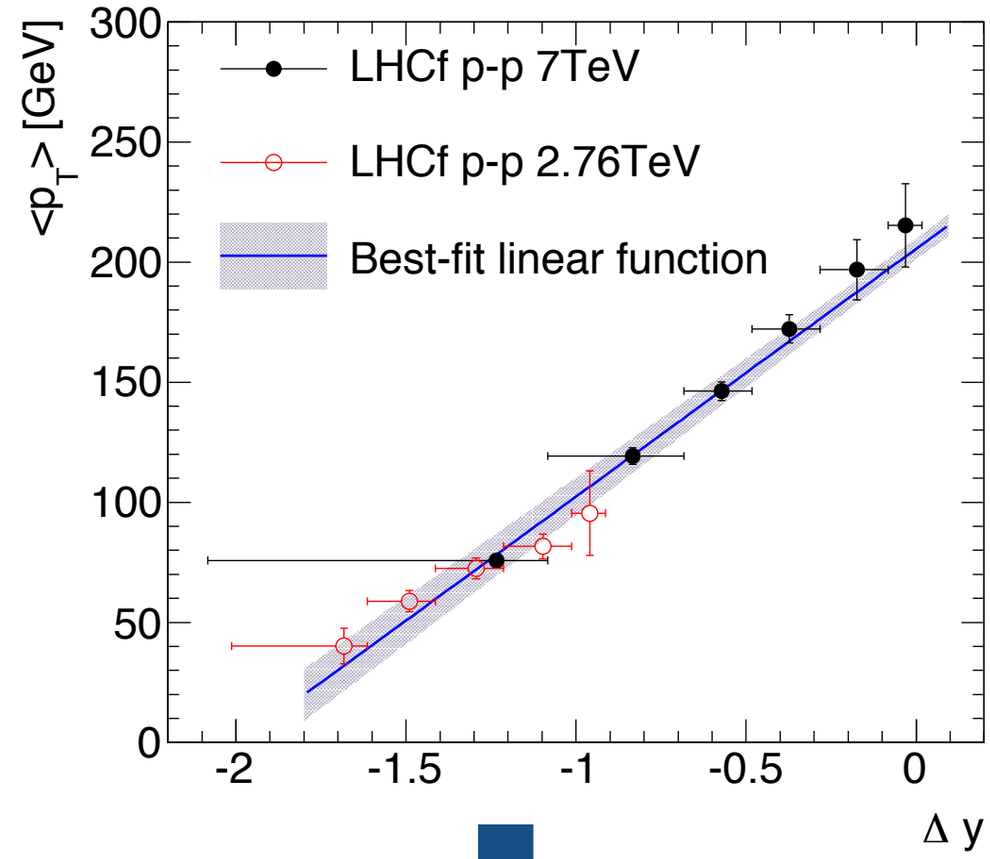

$(\Delta y \equiv y_{\rm beam} - y)$

1. Thermodynamics (Hagedron model)

$$\frac{1}{\sigma_{\rm inel}} E \frac{d^3\sigma}{dp^3} = A \cdot \exp(-\sqrt{{p_{\rm T}}^2 + m_{\pi^0}^2}/T)$$

$$\langle p_{\rm T} \rangle = \sqrt{\frac{\pi m_{\pi^0} T}{2}} \frac{K_2(m_{\pi^0}/T)}{K_{3/2}(m_{\pi^0}/T)}$$

2. Gauss distribution

$$\frac{1}{\sigma_{\rm inel}} E \frac{d^3\sigma}{dp^3} = A \cdot \frac{\exp(-p_{\rm T}^2/\sigma_{\rm Gauss}^2)}{\pi \sigma_{\rm Gauss}^2}$$

$$\langle p_{\rm T} \rangle = \frac{\sqrt{\pi}}{2} \sigma_{\rm Gauss}$$

$$\langle p_{\rm T} \rangle (y)|_{5.02{\rm TeV}} = 216.3 + 116.0(8.585 - y)\ [{\rm MeV}]$$

The p_T spectra in "p-p at 5.02TeV" are obtained by the Gauss distribution with the above $\langle p_T \rangle$ and absolute normalization.

arXiv:1403.7845, CERN-PH-EP-2014-059

Inclusive π^0 p_T spectra in p-Pb at 5.02TeV

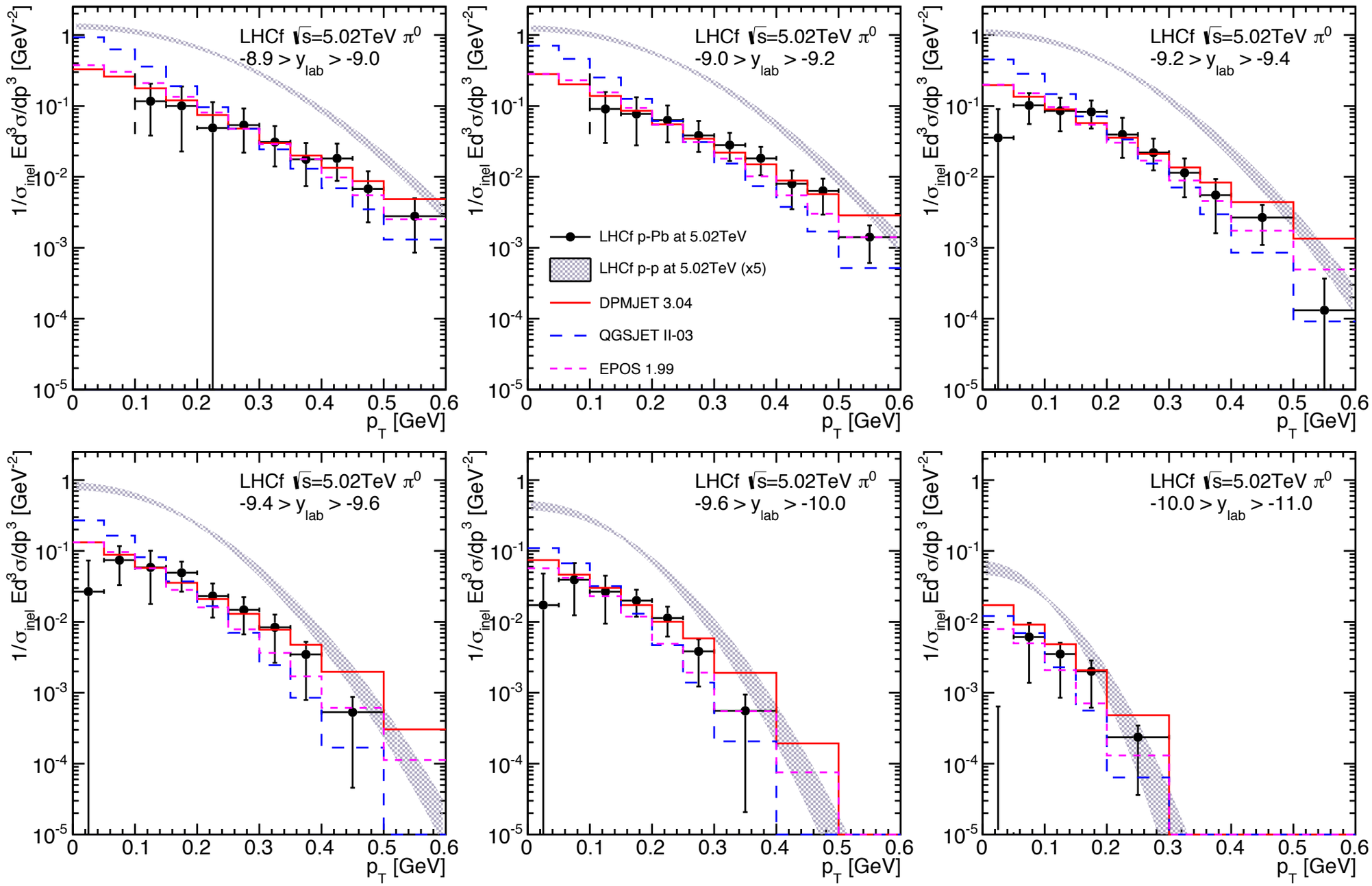

- The LHCf data in p-Pb (filled circles) show good agreement with DPMJET and EPOS.
- The LHCf data in p-Pb are clearly broadened than the LHCf data in p-p at 5.02TeV (shaded area). The latter is interpolated from the results at 2.76TeV and 7TeV.

arXiv:1403.7845, CERN-PH-EP-2014-059

Nuclear modification factor in p-Pb at 5.02TeV

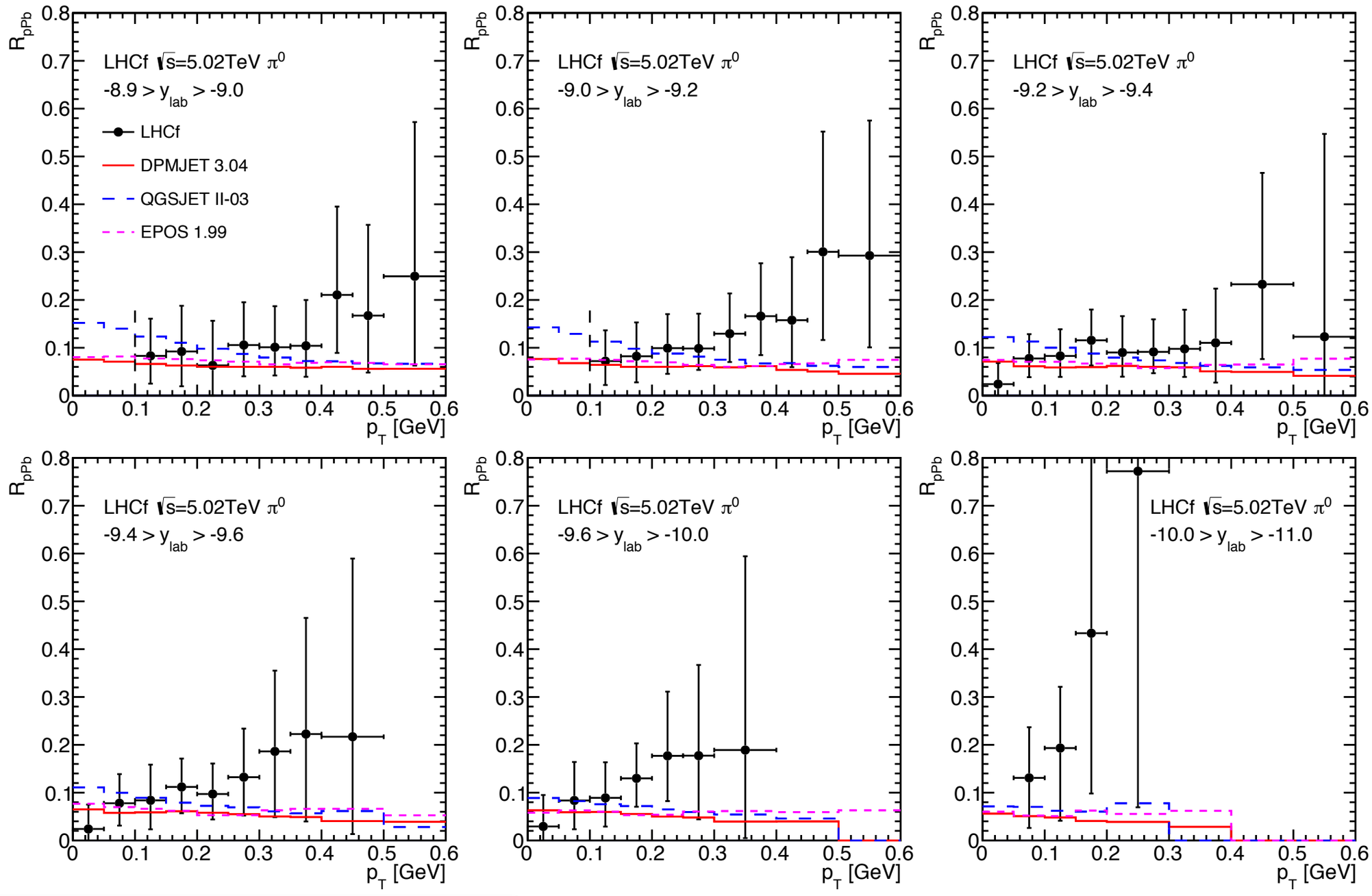

$$R_{\mathrm{pPb}}(p_{\mathrm{T}}) \equiv \frac{\sigma_{\mathrm{inel}}^{\mathrm{pp}}}{\langle N_{\mathrm{coll}}\rangle \sigma_{\mathrm{inel}}^{\mathrm{pPb}}} \frac{Ed^3\sigma^{\mathrm{pPb}}/dp^3}{Ed^3\sigma^{\mathrm{pp}}/dp^3}$$

$$\langle N_{\mathrm{coll}}\rangle = 6.9$$

- Both LHCf and MCs show strong suppression.
- LHCf grows as increasing p_T, which is understood by the softer p_T spectra in p-p at 5TeV than those in p-Pb.

Inclusive neutron energy spectra in p-p at 7TeV

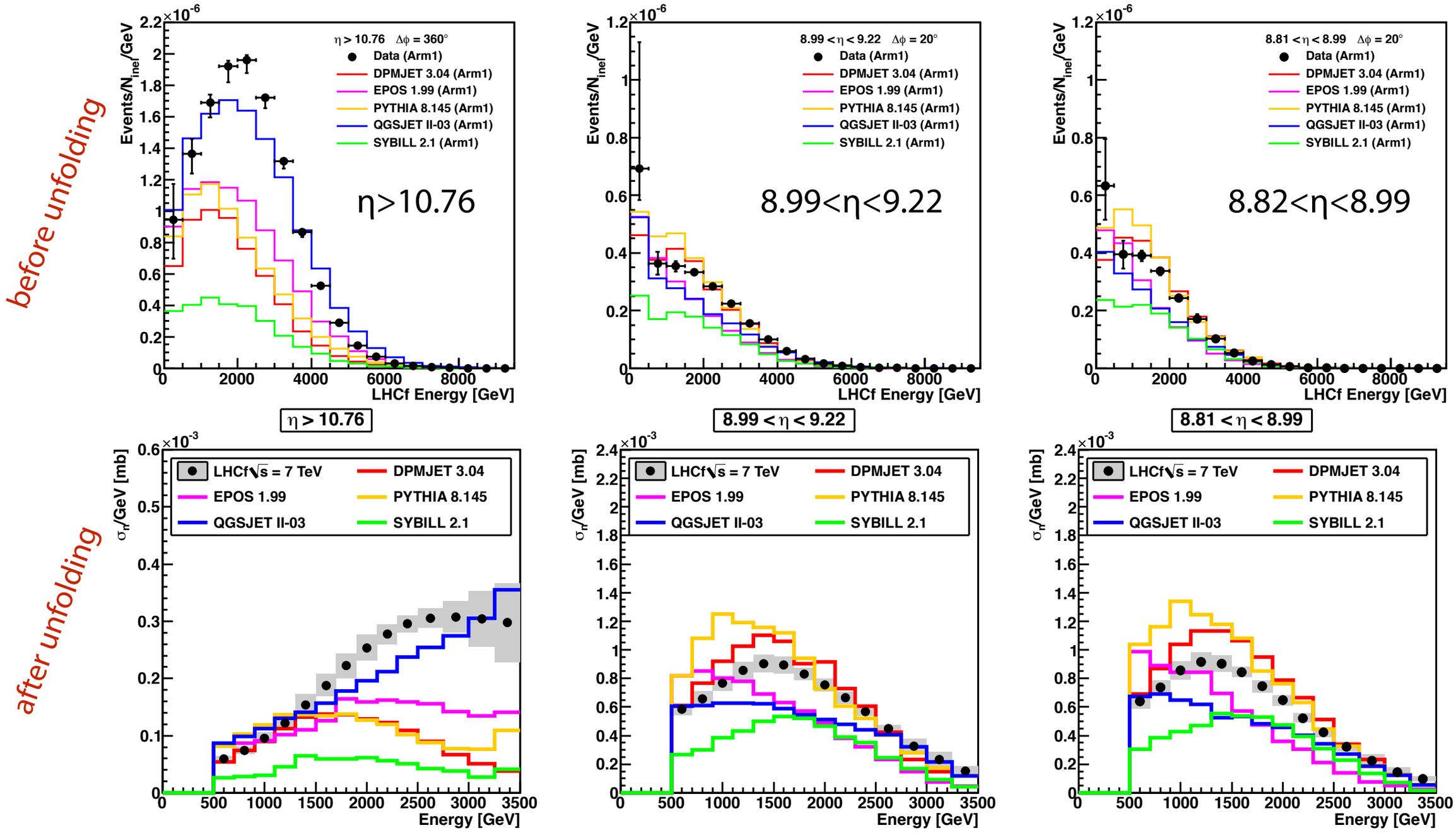

- In η>10.76 huge amount of neutron exists. Only QGSJET roughly reproduces the LHCf result.
- In other rapidity regions, the LHCf results are enclosed by the variation of models.
- These results may indicate small inelasticity in very forward region.

Towards the next operation at 13TeV

The LHCf detectors will be upgraded giving a priority to **high energy operation.**

1. Radiation damage will be more severe; 0.2Gy/nb^{-1} at 7TeV → 2-3Gy/nb^{-1} at 13TeV.
   - All of plastic scintillators were replaced with GSO scintillators in both Arm1 and Arm2. GSO scintillator can survive up to 10^6Gy.
   - Scintillation fibers (SciFi, position detector in Arm1) were replaced with GSO bars.
2. Old silicon detector would be saturated for >1.5TeV photon (Arm2).
   - New wire bonding scheme to avoid saturation effects, pulse height was reduced ~60%
   - Rearrangement of the Si detector position for effectively catching EM/hadon showers.

All parts except for new Si modules are ready and their properties were tested by the test beams at HIMAC (HI beam facility in Japan) and SPS.

p-p 7TeV ↓ p-Pb 5.02TeV, p-p 2.76TeV ↓ We are here ↓ p-p 13TeV ↓

	HIMAC Nov. 2011	HIMAC Jun. 2012	SPS Aug. 2012	HIMAC Jul. 2013	HIMAC Feb. 2014	LNS (Catania) Summer2014	SPS Oct. 2014
Arm1	GSO scinti.	GSO scinti. GSO bar (2/4)	GSO scinti. GSO bar (2/4)		GSO bar (4/4)		Full detector
Arm2		Old detector	Plastic scinti.	GSO scinti.		New Silicon	Full detector

Construction of GSO calorimeters

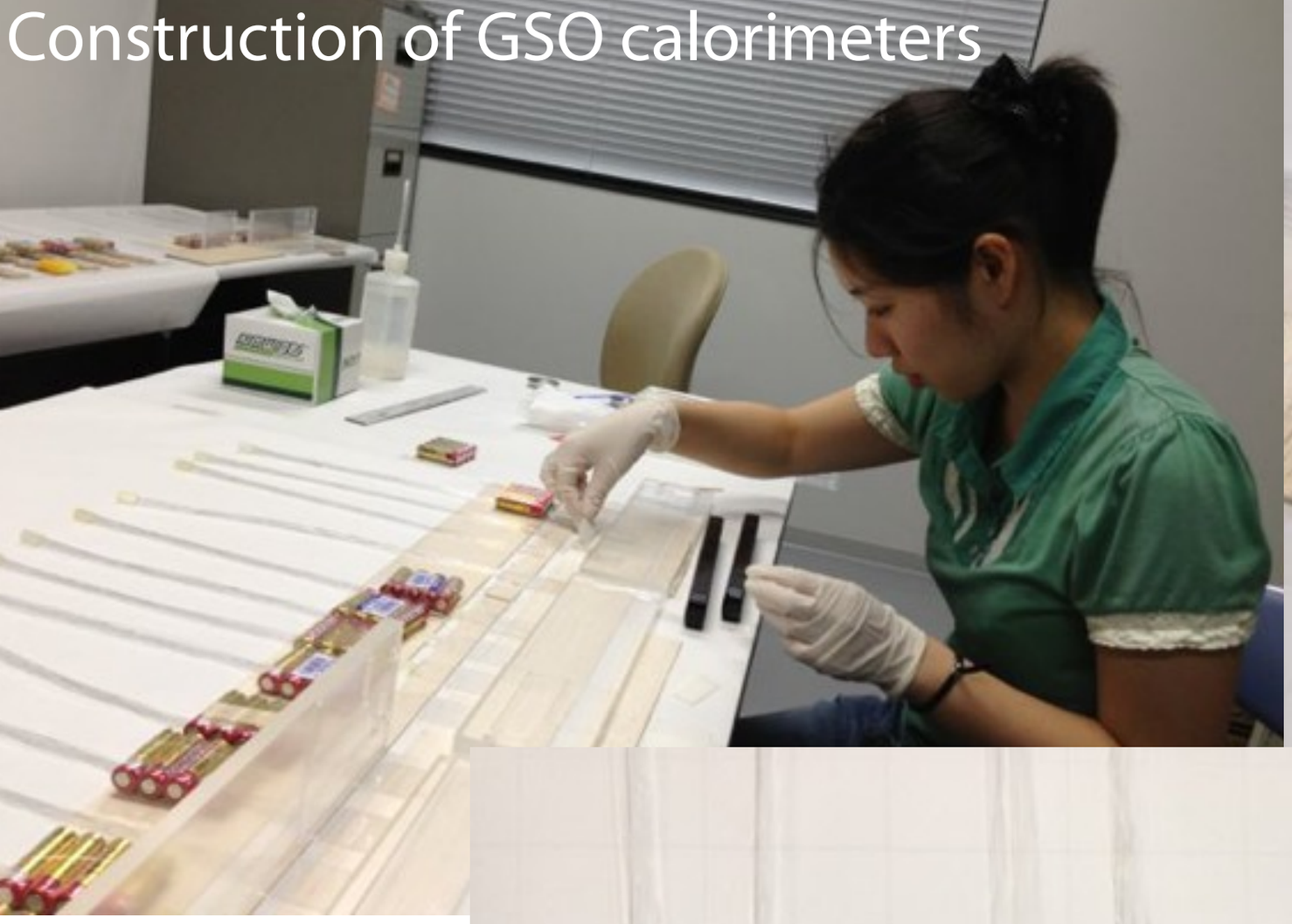

Wire bonding of Si sensor

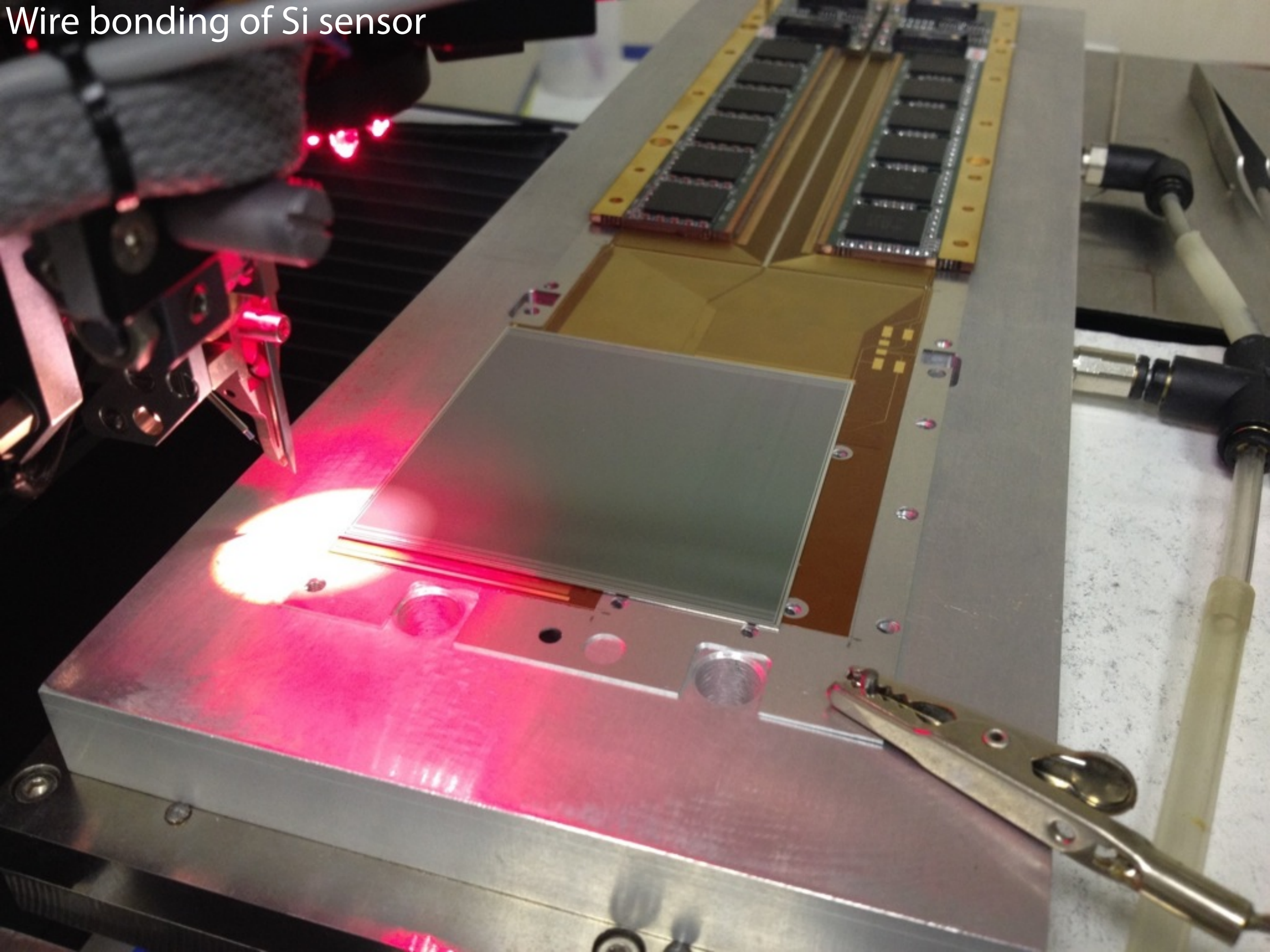

Summary

- Very forward π^0 production in p-Pb collision was measured at LHCf.
- Soft-QCD component of the measured π^0 production overall agree with DPMJET 3.04 and EPOS 1.99.
- Strong suppression of π^0 production is found in p-Pb collision which is consistent with predictions of DPMJET, EPOS and QGSJET II-03.

- Huge amount of neutron exists in very forward region, leading to small inelasticity.
- Detector upgrade is ongoing smoothly.

Backup

Prediction of X_{max} with retuned models

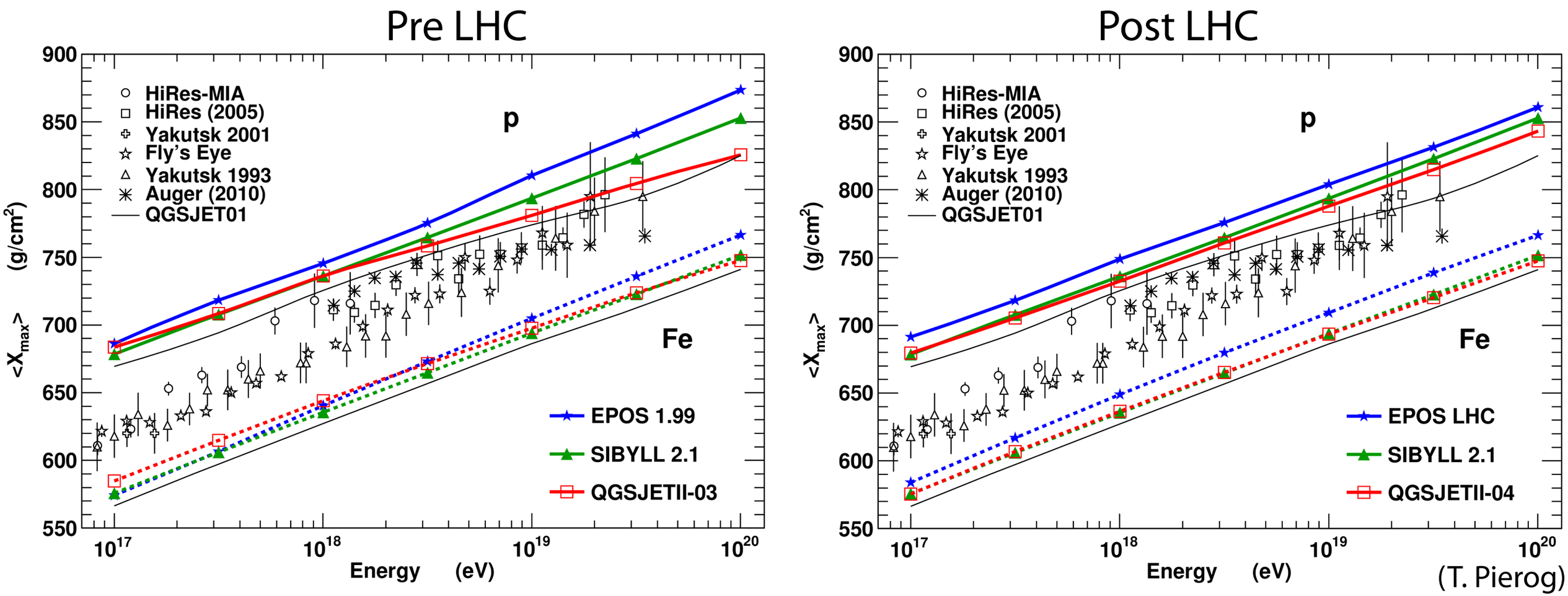

(T. Pierog)

- Difference of $\langle X_{max} \rangle$ in p-air among pre LHC models is about 50g/cm^2 at 10^{20}eV, although a difference between p-air and Fe-air is about 100g/cm^2.
- Retuned models with the the LHC data are somehow converged into pre-LHC model SIBYLL 2.1.
- Difference between p and Fe is reduced to 20g/cm^2.

Measurement of cosmic rays

- Direct* measurement (e.g. ballon, AMS etc.) of cosmic rays is quite severe above $E_{lab}=10^{14}$eV.
- Instead, indirect measurement observing cascade showers of daughter particles (extensive air-shower, EAS) is the best way to increase statistics.
- Largest systematic uncertainty of indirect measurement is caused by a finite understanding of the hadronic interaction of cosmic ray in atmosphere (because very high energy and very forward).

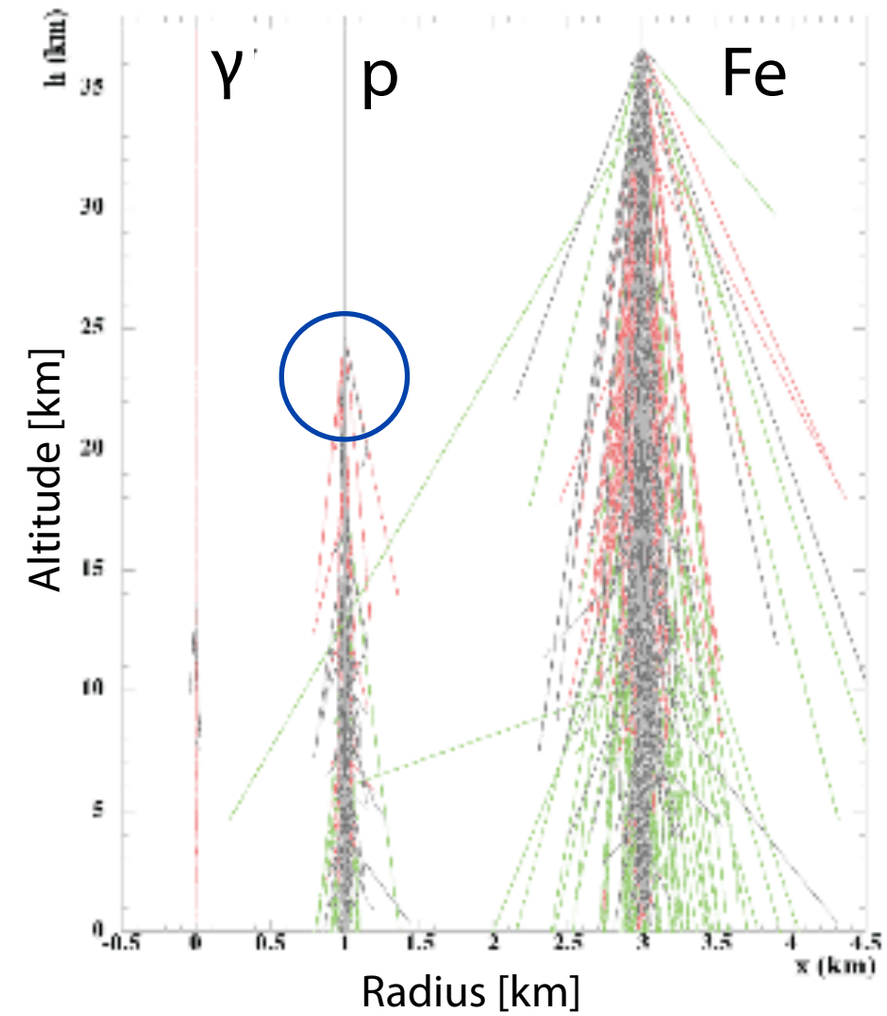

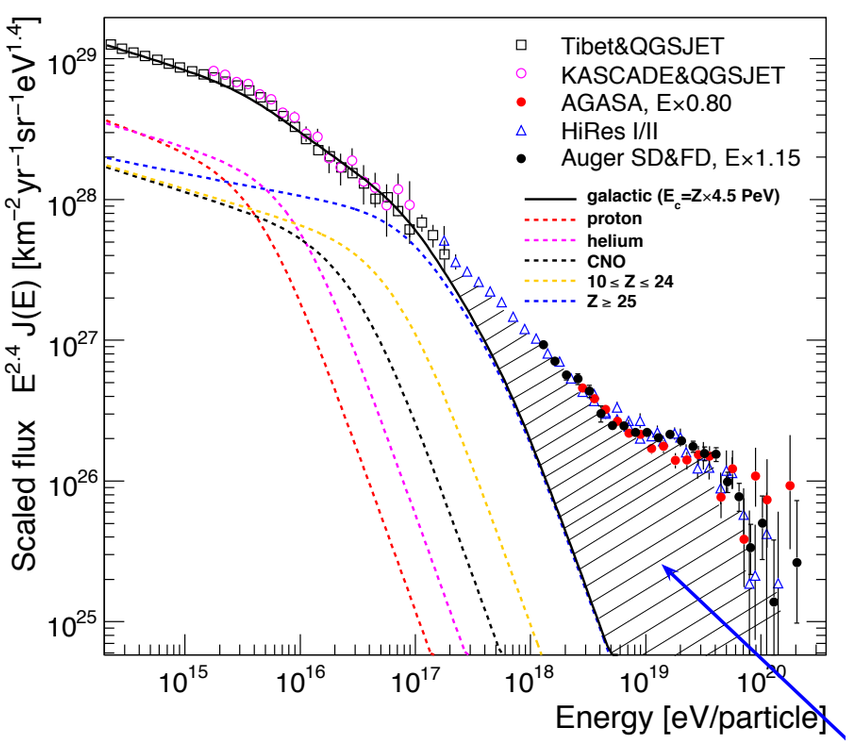

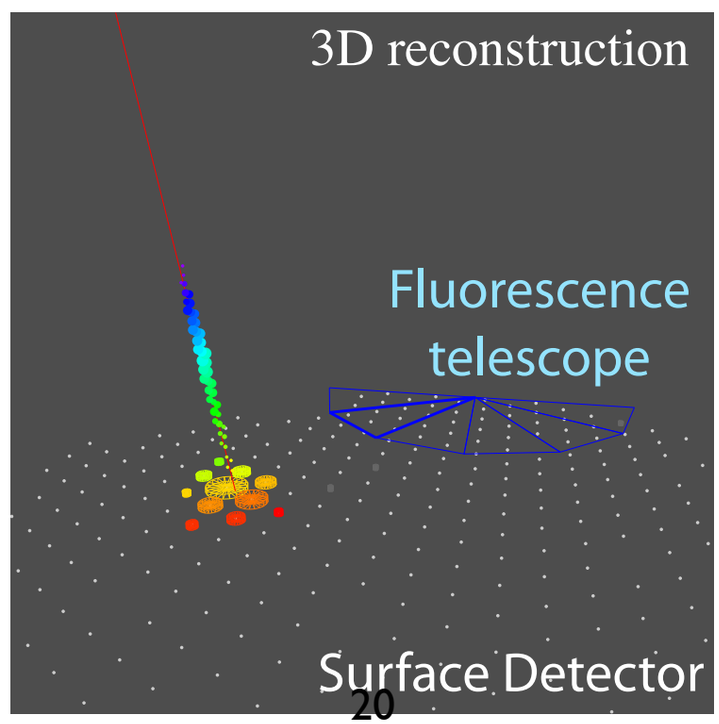

JINST 9 P03016 (2014)

Neutron event reconstruction

Neutron energy reconstruction

$$\sum_{l=2}^{15}$$

example at layer8th

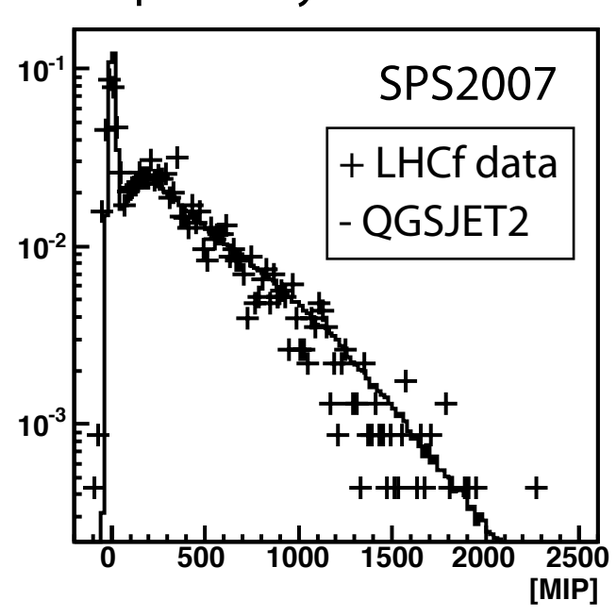

=

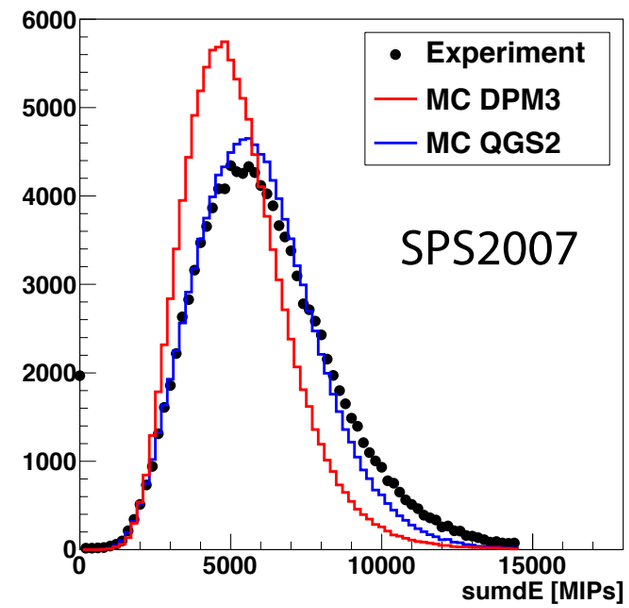

- Neutron energy is reconstructed by a sum of energy deposits.
- Detector simulation based on QGSJET2 for hadronic shower reproduces the test beam data better than that on DPMJET3.
- Difference between QGSJET2 and the test beam data is taken into account as a systematic error in the latter analysis.

Particle identification

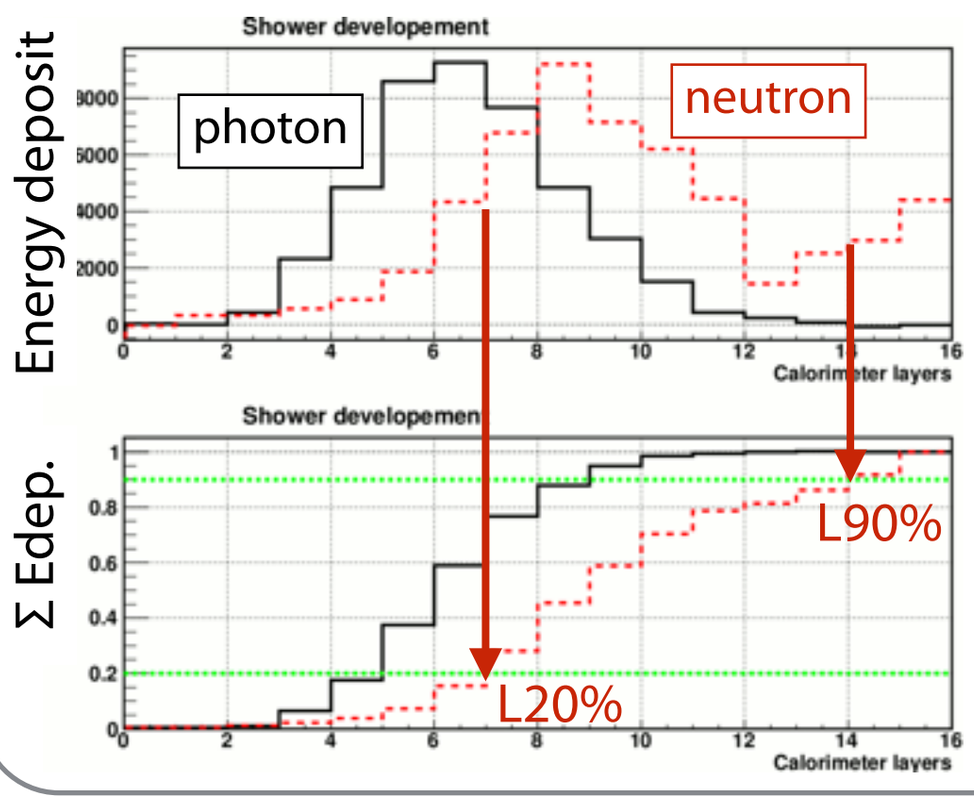

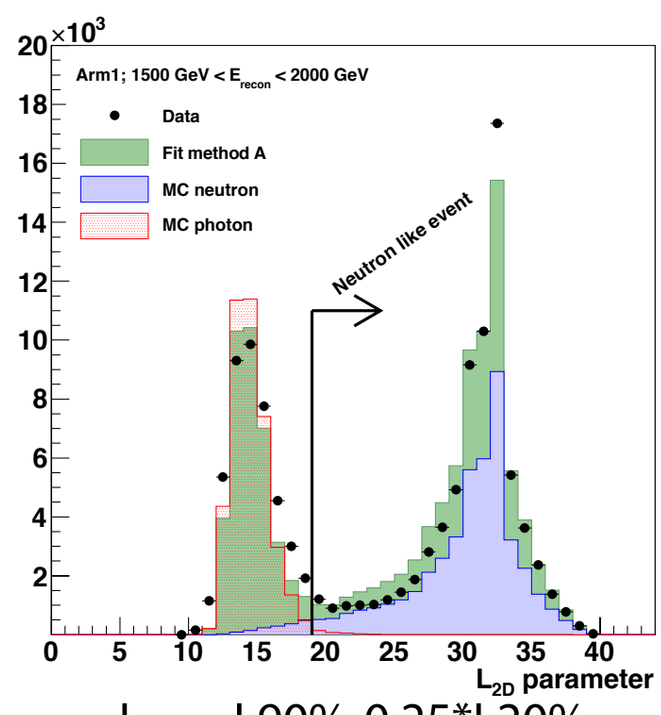

L_{2D} = L90%-0.25*L20%

- With two variables, L90% and L20%, PID performance is improved to reduce the photon contamination in neutron events.
- PID efficiency and purity are >90%.
- Energy spectra are corrected for PID inefficiency and BG contamination.

Results at the LHC: diffraction

Number of charged particles

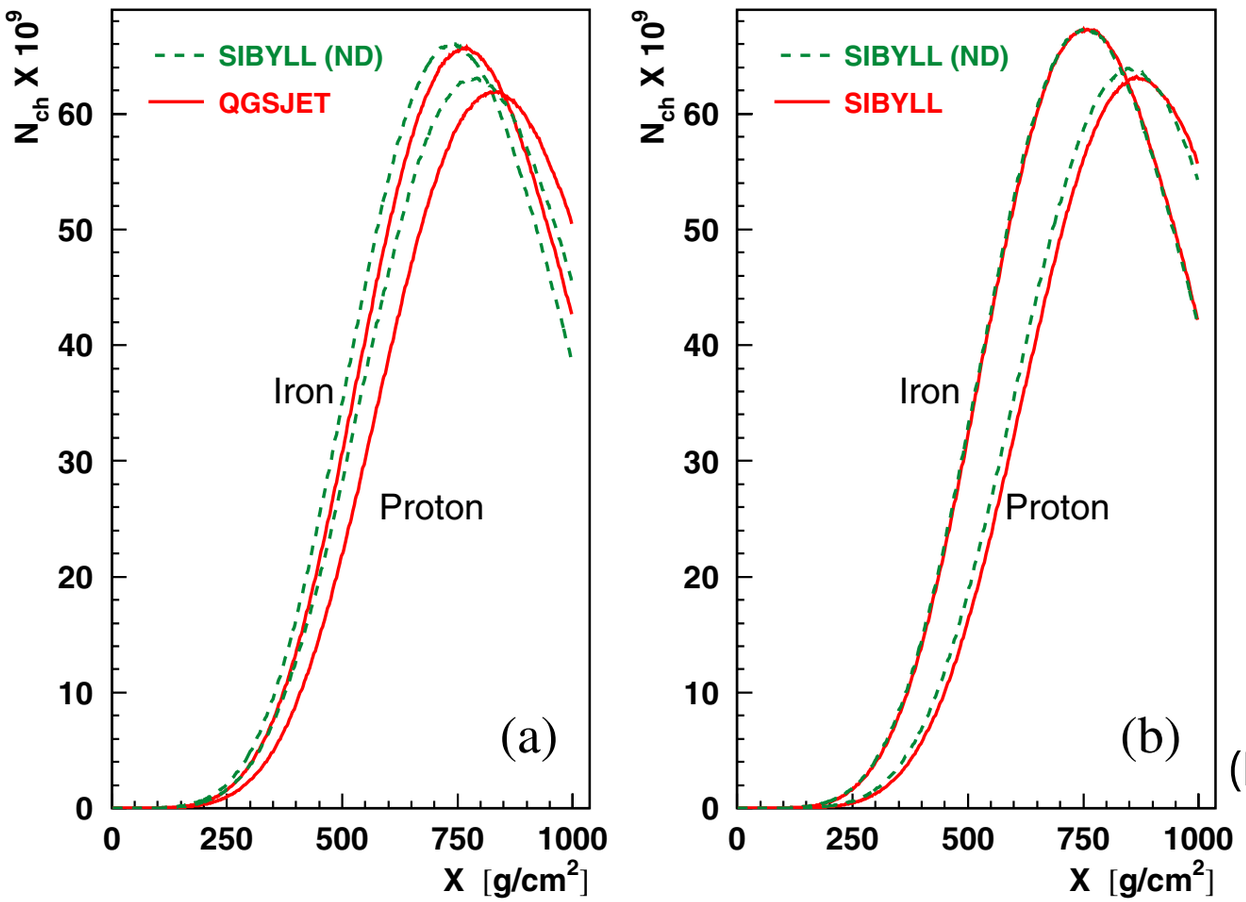

X_{max} of charged particles (dominantly electron) is insensitive to diffraction.

Number of muons

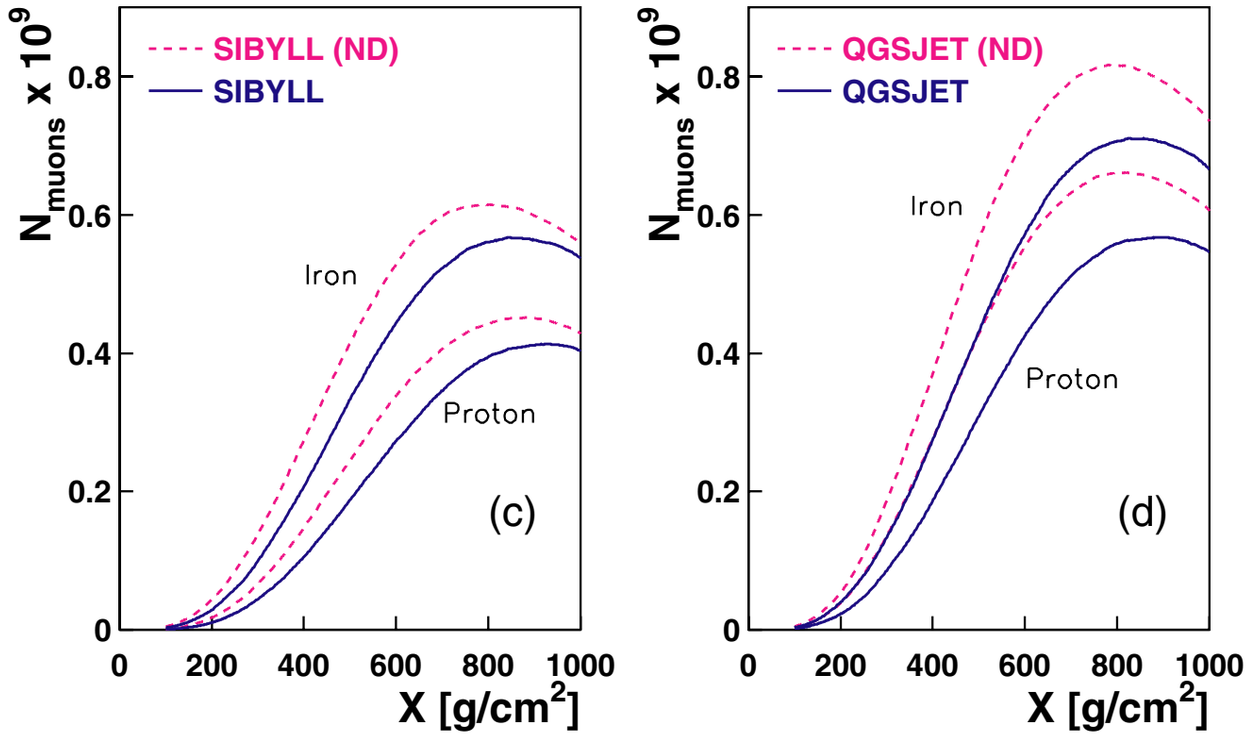

(R. Luna et al. PRD 70, 114034)

Muons are more sensitive to diffraction (i.e. leading baryon production): small multiplicity leading to less pions and less muons.

TOTEM Preliminary	$\sigma_{\rm SD} = 6.5 \pm 1.3 mb$
PYTHIA8	$\sigma_{\rm DD(4.7<\lvert\eta_{min}\rvert<6.5)} = 159 \mu b$
PHOJET	$\sigma_{\rm DD(4.7<\lvert\eta_{min}\rvert<6.5)} = 101 \mu b$
TOTEM (PRL101,262001)	$\sigma_{\rm DD(4.7<\lvert\eta_{min}\rvert<6.5)} = 116 \pm 25 \mu b$

Results at the LHC: cross section

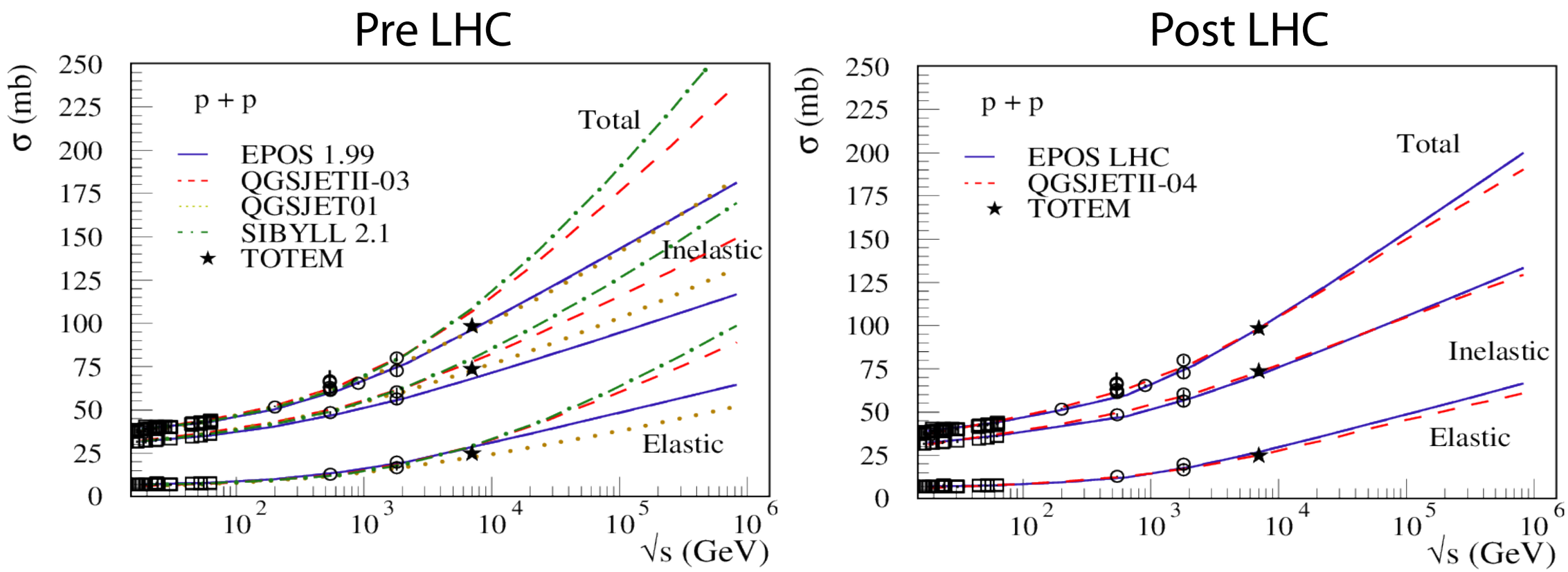

(T. Pierog)

- There is no drastic change from EPOS 1.99 to EPOS LHC.
- Better agreement with TOTEM is found in QGSJET II-04 compared with QGSJET II-03.
- Post LHC models show overall good agreement with data up to the LHC energy.
- They are converged into similar values even at 10^6GeV.

Extrapolation and scaling

Scaling of forward photon X_F distribution
(900GeV vs 7TeV)

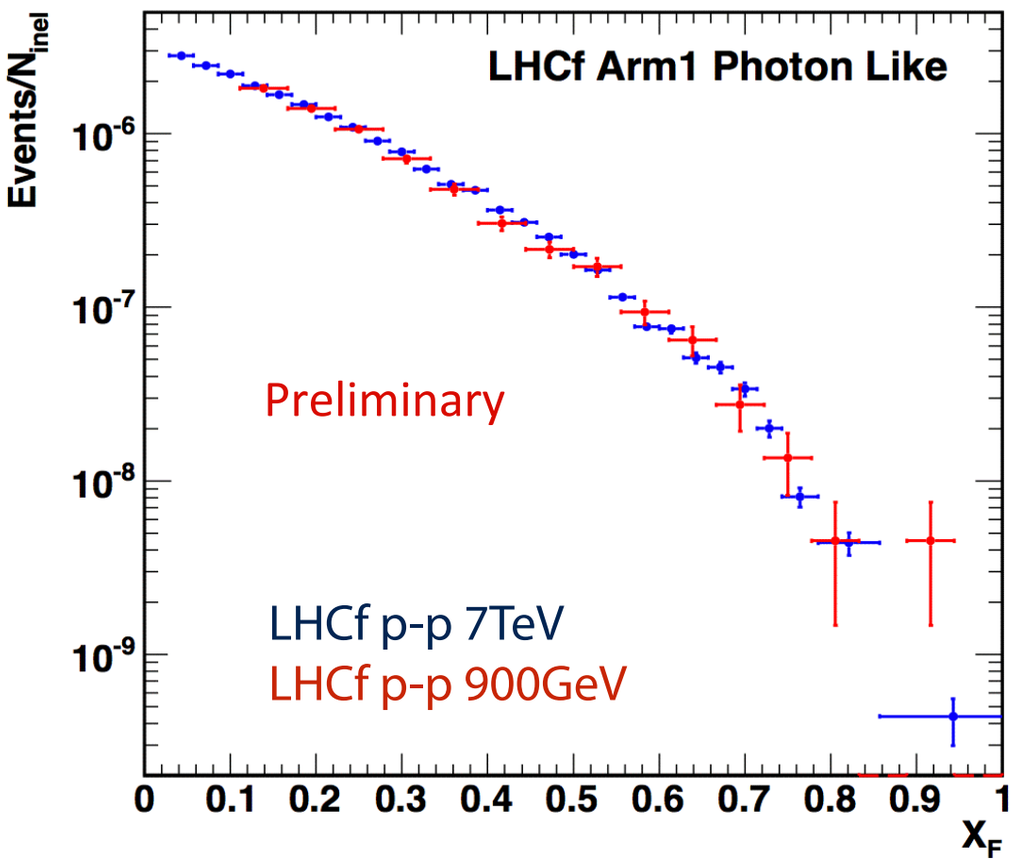

Scaling of forward π^0 average p_T
(2.76TeV vs 7TeV)

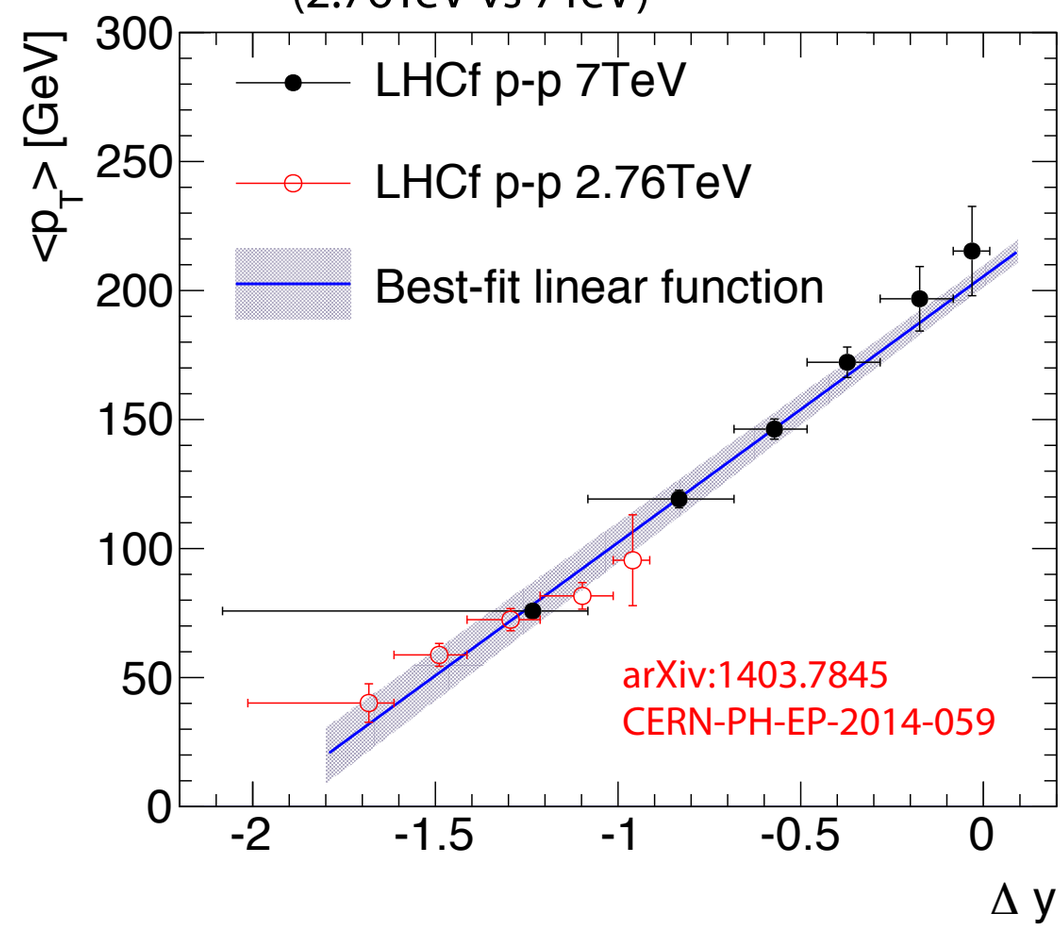

($\Delta y = y_{beam} - y$)

- Feynman scaling of forward photon energy and π^0 p_T distributions are found at LHCf.
- More precise extrapolation to ultrahigh energy.
  - LHC at 13 TeV
  - Extension to lower energy (e.g. RHIC at $\sqrt{s}$=510GeV).

The idea for the new silicon planes

In the original scheme one strip over two was connected to the front-end electronics and the other strips were floating.

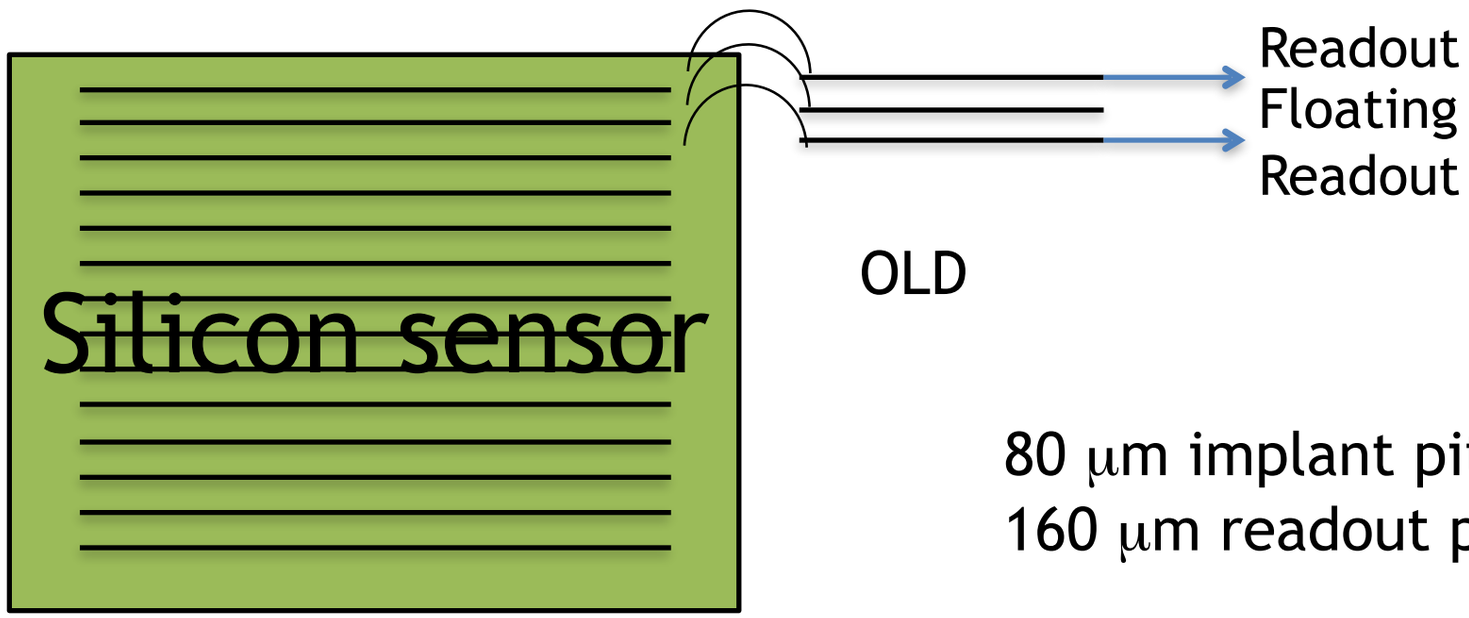

80 μm implant pitch
160 μm readout pitch

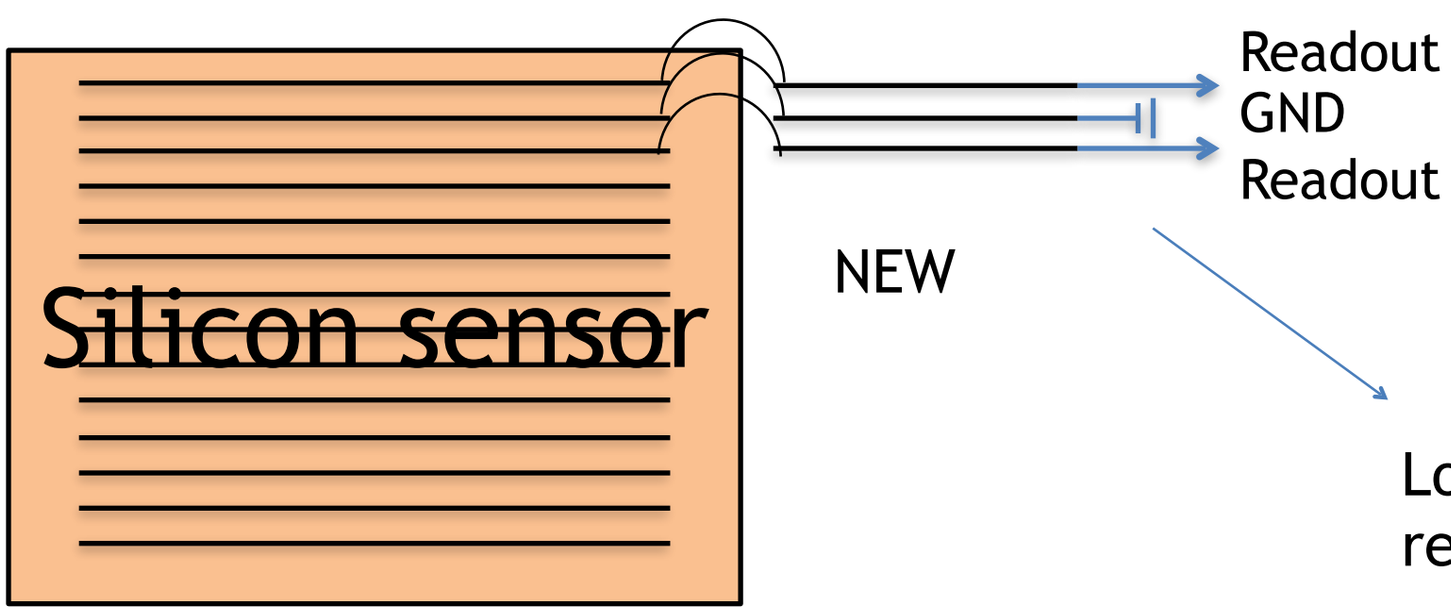

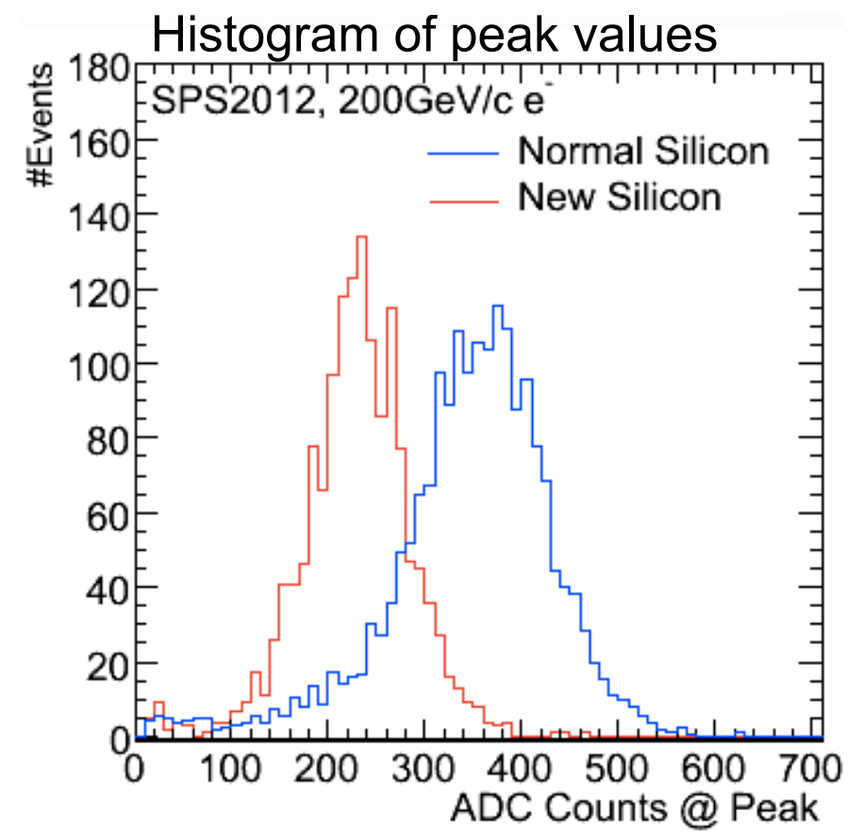

Loosing some part of the released energy

Assembling of new silicon planes

Gluing of **NEW** type hybrid circuits to old type kapton fanout

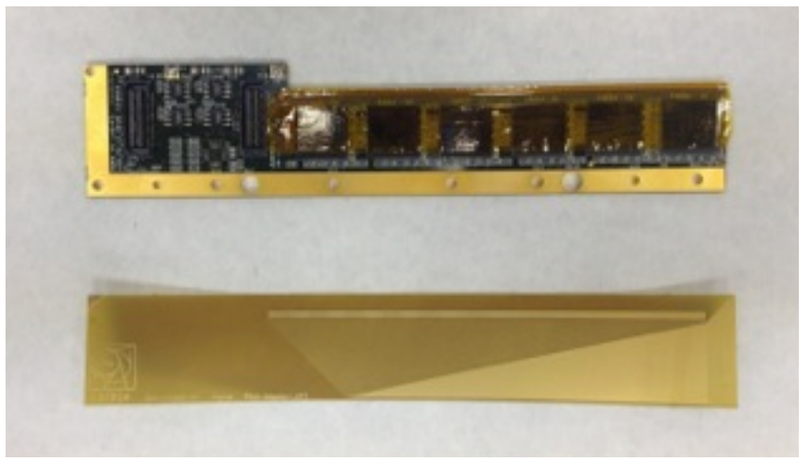

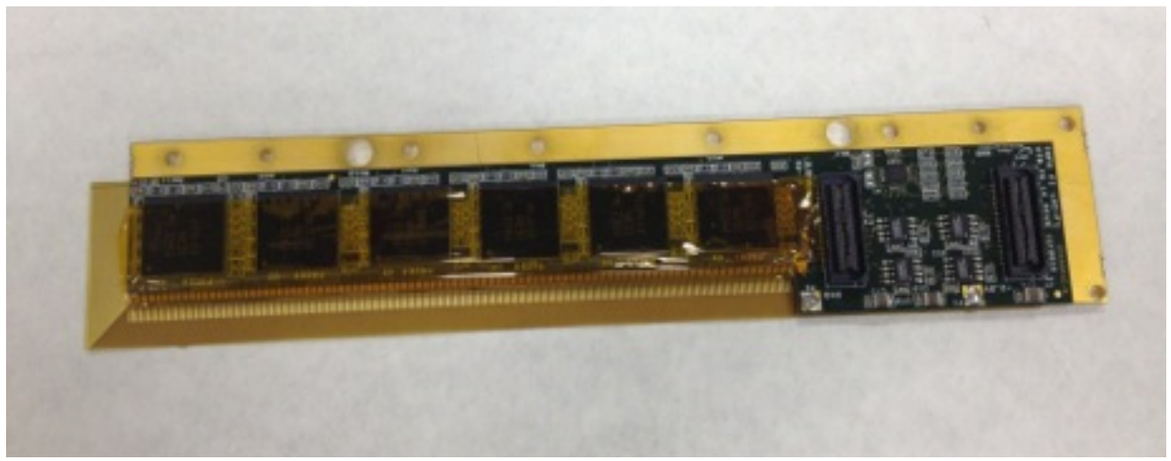

Gluing of silicon layers to the **NEW** kapton fanout (with GND pads for charge loss)

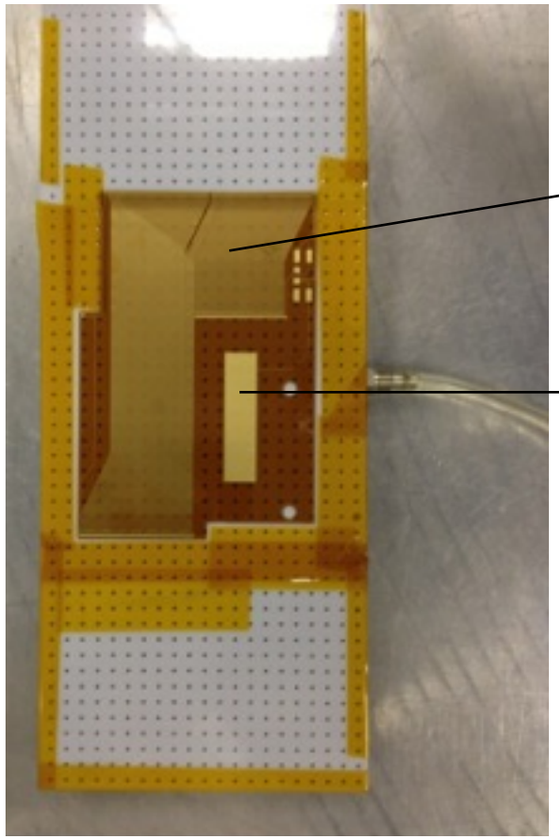

μ-strip fanout

Bias pad
(to be connected
to the silicon back-plane)

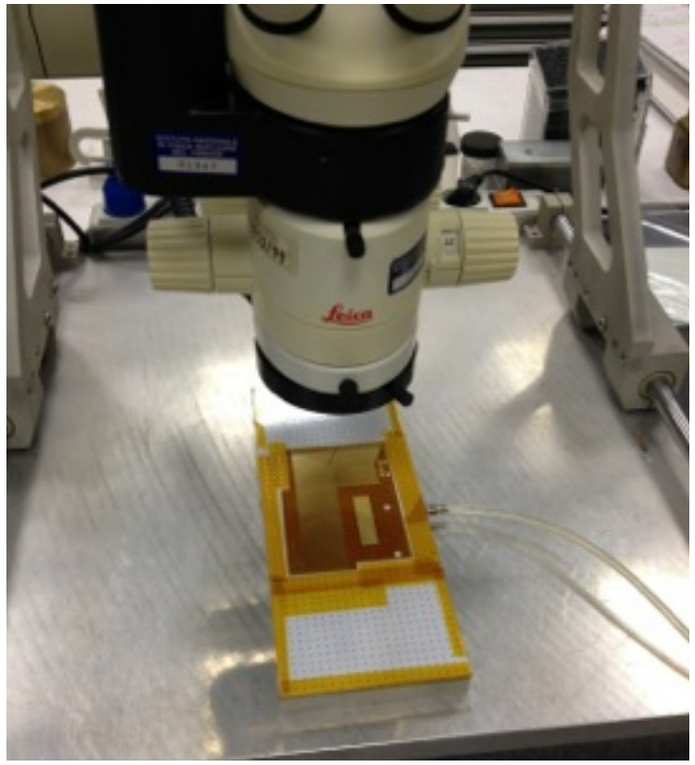

Glue deposition on the new kapton fanout cable

Plane with vacuum system

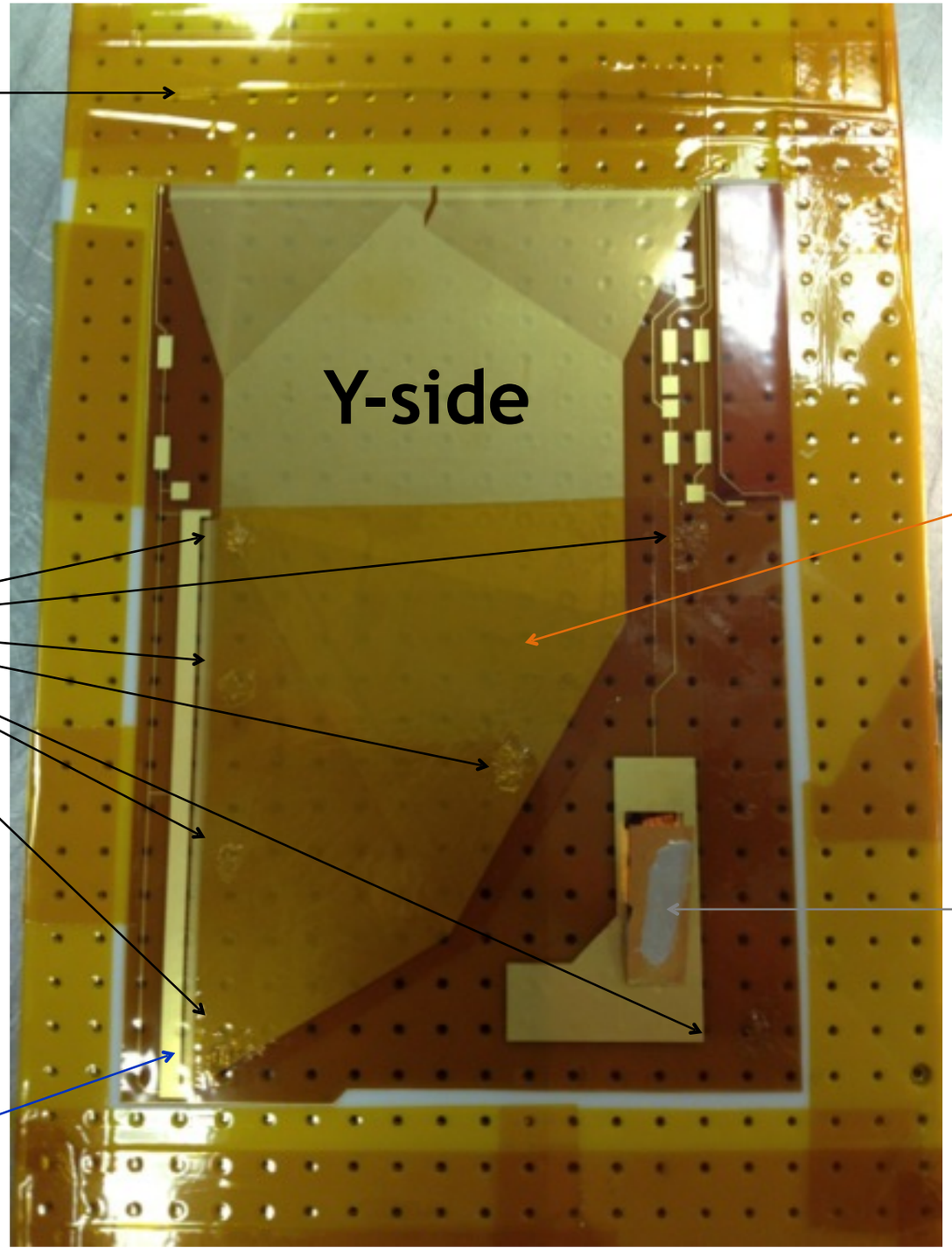

Thin layer of kapton tape for insulation

Thin layer of siliconic glue (not hard)

Electrically-conductive (Ag) glue deposited on a bent strip of golden kapton film for sensor biasing

GND large pad

Modification of the manipulators

Only one manipulator has been modified and tested.
The modification was necessary because the beam dumping procedure in 2013 went faster than in 2010. It lasted about 5 min. So the target of this modification was 5 min for 12 cm movement (from the operation position to the garage position it took about 12min before the modification)

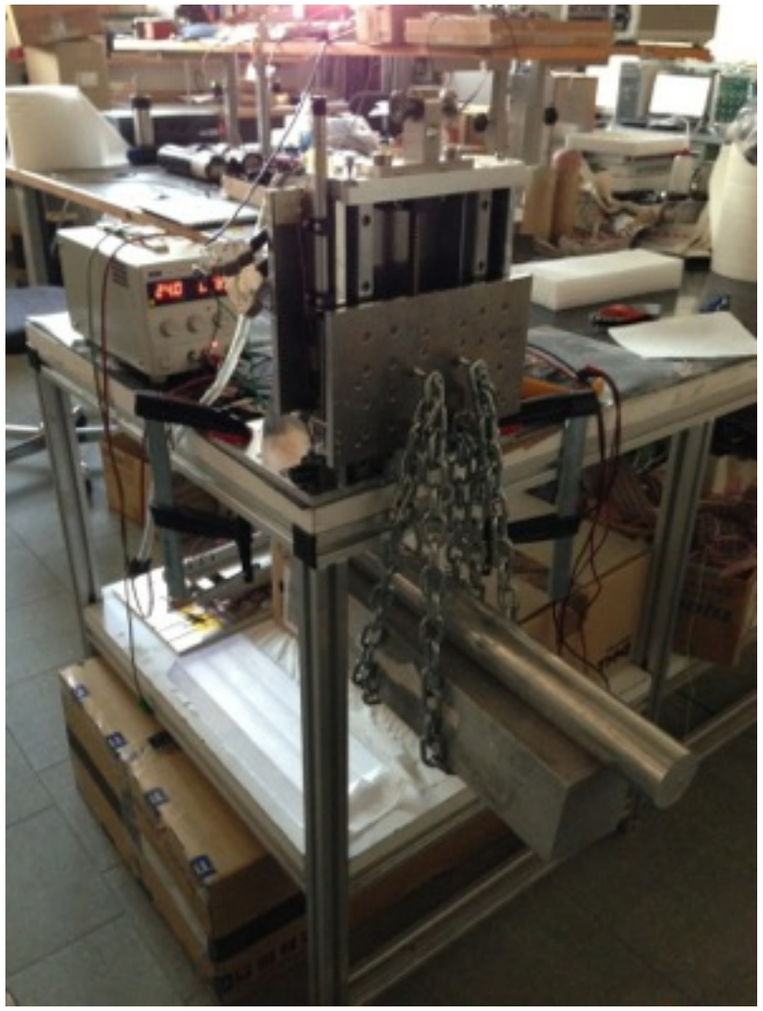

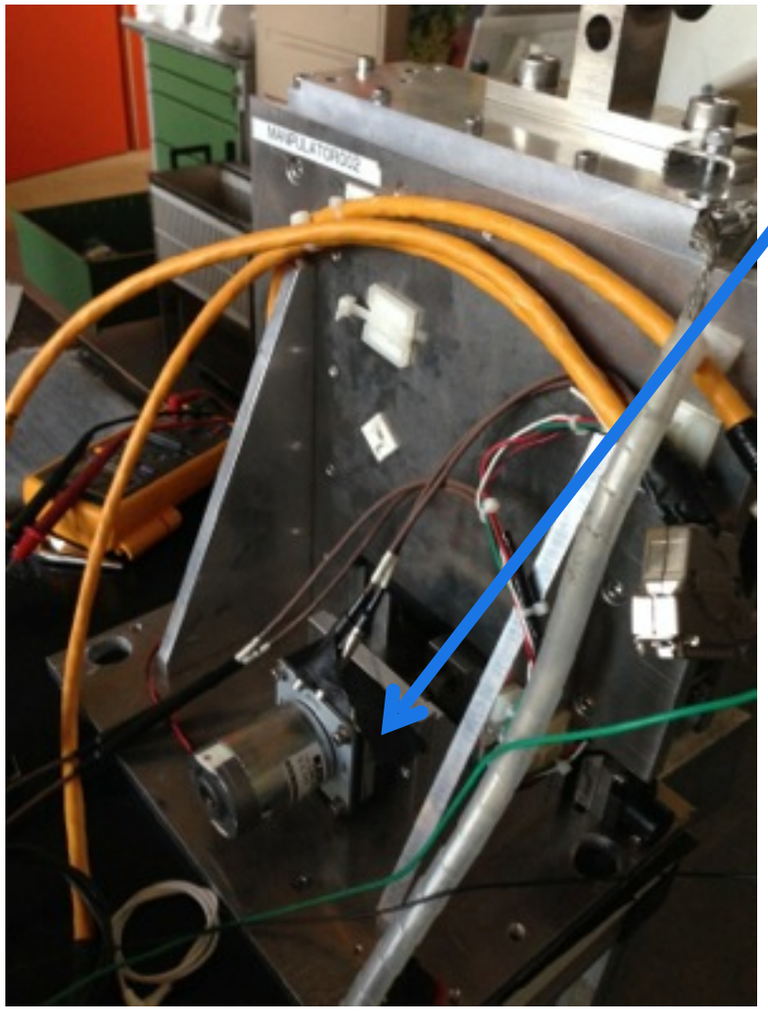

Replacement of the gear box (decreased the gear ratio from 30 to 12.5)

Test with the weight corresponding to the LHCf detector was successful.

Final vertical speed:
12 cm / 4 min

Power consumption is well below the limits of the engine